[15] Characterization of Lignin by ^{1}H and ^{13}C NMR Spectroscopy

By CHEN-LOUNG CHEN and DANIELLE ROBERT

Since 1951, rapid progress has been made in both the theory and experimental aspects of nuclear magnetic resonance (NMR). This is traceable to the fact that, unlike other forms of spectroscopy, the interpretation of NMR spectra in most cases is straightforward in terms of the fundamental parameters, such as chemical shifts, coupling constants, signal areas (intensities), and relaxation times. These parameters observed in NMR spectral experiments provide the necessary information for solving a wide variety of problems in the chemical and biological sciences.[1-5]

Most of the early work in NMR was focused on ^{1}H NMR spectroscopy. The major reason for this is that the ^{1}H nucleus, i.e., the proton, is the one most sensitive to NMR detection among the nuclei that give a NMR spectrum. However, the recent advances in Fourier transform NMR (FT-NMR) techniques lead to rapid development of the technique for obtaining natural abundance ^{13}C NMR spectra. Thus, ^{13}C NMR spectroscopy has become comparable to ^{1}H NMR spectroscopy in terms of importance as a tool for structural elucidation of organic substances, in spite of the low natural abundance of ^{13}C (1.1 at. %).

There are several advantages of ^{13}C NMR spectroscopy over ^{1}H NMR spectroscopy for the structural determination of organic compounds. In ^{13}C NMR, spectral data are obtained from the "backbone" of the molecule rather than from the exterior of the molecule as in ^{1}H NMR. Consequently, ^{13}C NMR spectrum of a compound provides information about the nature of all carbons in the molecules. In contrast, the corresponding ^{1}H NMR spectrum does not give information about the nature of quaternary carbons in the molecule, such as the carbons in R″-C(R′)= and $\rangle$C=O groups. The second advantage is that ^{13}C NMR spectra are not complicated by spin–spin coupling. The probability of having two ^{13}C

[1] J. M. Emseley, J. Feenay, and L. H. Sutcliffe, "High Resolution Nuclear Magnetic Resonance Spectroscopy," Vol. I. Pergamon, London, England, 1967.

[2] E. Breitmaier, and W. Voelter, "Carbon-13 NMR Spectroscopy," 3rd Ed. VCH, Weinheim, Federal Republic of Germany, 1987.

[3] D. E. Leyden, and R. H. Cox, "Analytical Applications of NMR." Wiley, New York, 1977.

[4] R. J. Abraham, and P. Loftus, "Proton and Carbon-13 NMR Spectroscopy." Heyden & Son, Sussex, England, 1979.

[5] R. K. Harris, "Nuclear Magnetic Resonance Spectroscopy." Pitman, Marshfield, Massachusetts, 1983.

nuclei adjacent to each other in the same molecule is so low (1/10,000) that the possibility of $^{13}C-^{13}C$ coupling can be ignored. Moreover, ^{13}C NMR spectra are usually obtained with broadband noise, proton decoupling,[6] so that only single signals are observed for each ^{13}C resonance. The third advantage is that the ^{13}C NMR chemical shift range of the majority of diamagnetic organic compounds is about 240 ppm (in δ scale) in comparison with about 12 ppm for ^{1}H NMR. All these imply that there is better resolution and less overlap of signals in ^{13}C NMR spectra of organic compounds, particularly of polymeric natural products, such as lignin, than the corresponding ^{1}H NMR spectra. In addition, there is a greater probability of observing individual carbon resonances. One of the disadvantages of ^{13}C NMR spectroscopy over ^{1}H NMR spectroscopy is that routine ^{13}C NMR spectra are not quantitative. The area under each signal in a routine ^{13}C NMR spectra is not proportional to the number of the corresponding ^{13}C nuclei giving rise to these signals because of the nuclear Overhauser effect (NOE) and the different relaxation times of the different carbon. In order to obtain a quantitative ^{13}C NMR spectrum of an organic compound, a specific pulse sequence is required. The other disadvantage is that the ^{13}C nucleus is significantly less sensitive than the ^{1}H nucleus toward magnetic field, relative sensitivity of 0.00018 versus 1 in a constant magnetic field at natural isotopic abundance.

Among the various physical and chemical methods for characterization of lignins, ^{1}H NMR[7-10] and ^{13}C NMR[11-16] spectroscopy has been shown to be among the most reliable and comprehensive techniques. The characterization of lignin by ^{13}C NMR spectroscopy, in particular, furnishes rather comprehensive data about the nature of all carbons in lignin in terms of chemical structure. By contrast, the other physical and chemical analytical methods only provide incomplete information on the chemical structure of lignin (see chapter [14] in this volume). However, several difficulties are still encountered in the interpretation of the ^{1}H NMR and ^{13}C NMR spectra of lignins, e.g., the assignment of signals, because of the intensive

[6] R. R. Ernst, *J. Chem. Phys.* **45**, 3845 (1966).
[7] C. H. Ludwig, B. L. Nist, and J. L. McCathy, *J. Am. Chem. Soc.* **86**, 1186 (1964).
[8] C. H. Ludwig, B. L. Nist, and J. L. McCathy, *J. Am. Chem. Soc.* **86**, 1196 (1964).
[9] A. Klemola, *Suom. Kemistil. B* **41**, 99 (1968).
[10] K. Lundquist, *Acta Chem. Scand., Ser. B* **35**, 497 (1981).
[11] H.-D. Lüdemann and H. Nimz, *Makromol. Chem.* **175**, 2409 (1974).
[12] H. Nimz, I. Mogharab, and H.-D. Lüdemann, *Makromol. Chem.* **175**, 2563 (1974).
[13] H. Nimz, D. Robert, O. Faix, and M. Nemr, *Holzforschung* **35**, 16 (1981).
[14] C.-L. Chen, M. G. S. Chua, J. Evans, and H.-M. Chang, *Holzforschung* **36**, 239 (1982).
[15] C. Lapierre, J. Y. Lallemand, and B. Monties, *Holzforschung* **36**, 275 (1982).
[16] K. P. Kringstad and R. Mörck, *Holzforschung* **37**, 237 (1983).

overlap of signals for ^{1}H and ^{13}C nuclei in lignin present in similar, but nonidentical chemical environments. Some of these difficulties can be circumvented by the application of more sophisticated ^{13}C NMR pulse sequences[13] such as the attached proton test (APT) experiment,[17,18] and the distortionless enhancement by polarization transfer (DEPT) sequence.[18-22] The DEPT pulse sequence is particularly suitable for characterization of lignins by ^{13}C NMR spectroscopy, overcoming the loss of information caused by proton decoupling.[23,24] This pulse sequence is a one-dimensional pulse sequence, involving spin echo phenomenon to observe separately signals for ^{13}C nuclei of CH, CH_2, and CH_3 groups; hence, the multicity of ^{13}C NMR signals can be unambiguously determined. [In addition, the pulse sequence significantly induces the enhancement of signal intensity due to the polarization transfer involving a spin population interchange between the more sensitive nucleus (^{1}H) and the less sensitive nucleus (^{13}C) to the benefit of the latter.] This chapter deals with the characterization of lignin by ^{1}H and ^{13}C NMR spectroscopy. The latter includes techniques for obtaining routine, quantitative, and DEPT ^{13}C NMR spectra of lignins. Before describing the aforementioned procedures, the principle of NMR spectroscopy will be presented.

Pulse Fourier Transform NMR Techniques[1-5]

One of the important limitations of NMR spectroscopy is the low sensitivity of the method as compared to other spectroscopic techniques, such as infrared and ultraviolet-visible spectroscopy. The major cause for the low sensitivity is traceable to the very small magnitude in the energy changes (in the order of about 10^{-2} cal/mol) involved in NMR transitions. Moreover, the low natural abundance of some nuclei, such as ^{13}C and ^{35}Cl, in nature makes observation of NMR signals for these nuclei on a routine NMR procedure, e.g., continuous wave (CW) technique, using natural abundance samples, even more difficult. One of the most effective methods to overcome this difficulty is the pulsed Fourier transform (FT) NMR technique.

[17] D. L. Robenstein and T. T. Takashima, *Anal. Chem.* **51,** 1465A (1979).
[18] S. L. Patt and J. N. Shoolery, *J. Magn. Reson.* **46,** 535 (1982).
[19] D. M. Doddrell, D. T. Pegg, and M. R. Bendall, *J. Magn. Reson.* **48,** 323 (1982).
[20] D. M. Doddrell, D. T. Pegg, and M. R. Bendall, *J. Chem. Phys.* **77,** 2745 (1982).
[21] O. W. Sorensen and R. R. Ernst, *J. Magn. Reson.* **51,** 477 (1983).
[22] R. Benn and H. Gunther, *Angew. Chem., Int. Ed. Engl.* **22,** 350 (1983).
[23] C. Lapierre, B. Monties, E. Guittet, and J. Y. Lallemand, *Holzforschung* **38,** 333 (1984).
[24] M. Bardet, M.-F. Foray, and D. Robert, *Makromol. Chem.* **186,** 1495 (1985).

Nuclear Magnetic Resonance

When a nucleus with spin quantum number $I \neq 0$ is placed in a constant magnetic field B_0, the magnetic moment takes up one of the allowed orientations of an angle θ to the direction of the magnetic field, as shown in Fig. 1. The magnetic moment μ will then experience a torque L tending to align it parallel to the field. However, since the nucleus is spinning, the torque causes μ to precess about the magnetic field B_0. According to Newton's law, the rate of change of angular momentum p with time is equal to the torque L.

$$dp/dt = L \tag{1}$$

From magnetic theory

$$L = \mu B_0 \tag{2}$$

Substituting Eq. (2) into Eq. (1), then

$$dp/dt = \mu B_0 \tag{3}$$

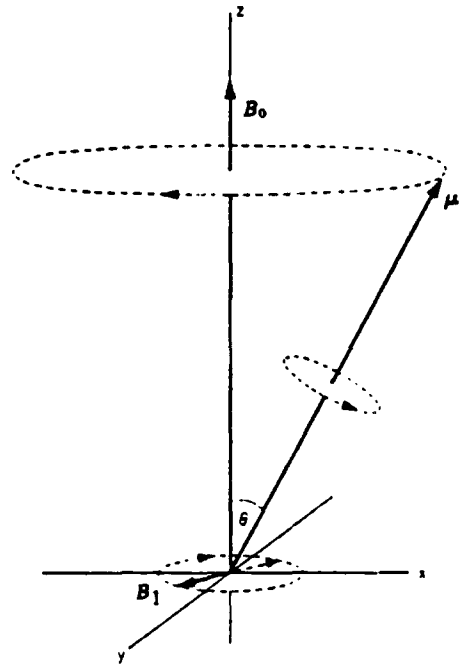

FIG. 1. Classical Larmor precession.[1] (Reproduced by permission of Pergamon, Oxford, England.)

Since $\gamma = \mu/p$ where γ is the magnetogyric ratio, Eq. (3) becomes

$$dp/dt = \gamma p B_0 \tag{4}$$

This equation of motion describes the precession of p about B_0 with angular frequency ω_0 defined by

$$dp/dt = p\,\omega_0 \tag{5}$$

hence,

$$\omega_0 = \gamma\, B_0 \tag{6}$$

Since $\omega_0 = 2\pi\nu_0$ by definition, Eq. (5) can be rewritten in terms of the precession frequency ν_0

$$\nu_0 = (\gamma/2\pi)\, B_0 \tag{7}$$

This equation is called the Larmor equation. An important point regarding this equation is that the frequency ν_0 is independent of the angle of inclination of the nuclear axis to the direction of the field.

If a secondary smaller magnetic field B_1 is applied perpendicular to the direction of the magnetic field B_0, i.e., x–y plane in the stationary frame of reference, and rotating about B_0 in the same direction as μ, then interactions between B_1 and μ occur. In practice, the rotating field B_1 is obtained by passing an alternating current through a coil. The coil is mounted perpendicular to the direction of B_0 in order to produce a magnetic field oscillating along the x-axis in the stationary frame of reference. An application of voltage to the coil at frequency $\omega = 2\pi\nu$ produces two equal counterrotating fields, having vectors in the magnitudes ($B_1 \cos \omega t + B_1 \sin \omega t$) and ($B_1 \cos \omega t - B_1 \sin \omega t$), as shown in Fig. 2. When the frequency of the rotating field B_1, $\nu = \omega/2\pi$, is equal to the precession frequency ν_0 of the magnetic moment μ, the nucleus absorbs energy from B_1, causing the magnetic moment to change the orientation with respect to the direction of the magnetic field B_0. This transition of energy states is called NMR phenomenon. At a magnetic field of 46,974 gauss, the Larmor

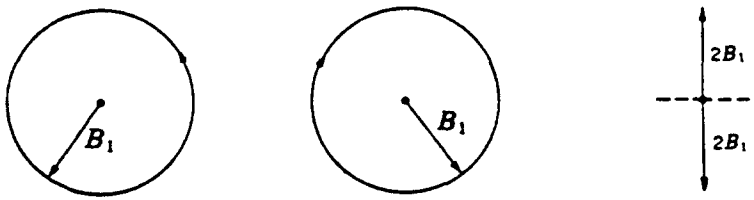

FIG. 2. A schematic illustration of the rotating magnetic field B_1.[1] (Reproduced by permission of Pergamon, Oxford, England.)

frequencies for ^1H and ^{13}C nuclei are in the range of 200 and 50.28 MHz, respectively.

Nuclear Energy Levels and Boltzmann Distribution

The energy E for a magnetic moment μ of a nucleus with spin quantum number I in a constant magnetic field B_0 is given by

$$E = m\gamma(h/2\pi)B_0 \tag{8}$$

where m is magnetic quantum number and has values $-I, -I+1, \ldots, I-1, I$. Thus, the magnetic moment has $2I+1$ energy levels.

For an assembly of identical nuclei with $I = \frac{1}{2}$. e.g., ^1H and ^{13}C nuclei, there are two allowed orientations, i.e., energy levels (Fig. 3), for their magnetic moments with respect to the direction of a constant magnetic field, when the nuclei are placed in the field. From Eq. (8), E for the magnetic moment at the lower energy level $m = -\frac{1}{2}$ (α state) is

$$E_\alpha = -\gamma(h/4\pi)B_0 \tag{9}$$

and E for the magnetic moment at the upper energy level $m = \frac{1}{2}$ (β state) is

$$E_\beta = \gamma(h/4\pi)B_0 \tag{10}$$

The selection rule allows the transition of energy only when $m = \pm 1$. Thus, at the NMR condition, the transition energy ΔE is

$$\Delta E = E_\alpha - E_\beta = \gamma(h/2\pi)B_0 \tag{11}$$

Moreover, according to the selection rule $\Delta m = \pm 1$, there are two allowed transitions: (1) from the α state to the β state with $\Delta m = 1$, which corresponds to an absorption of energy, and (2) from the β state to the α state with $\Delta m = -1$, which corresponds to induced emission, as shown in Fig. 3. Since the coefficients for absorption and induced emission of energy are

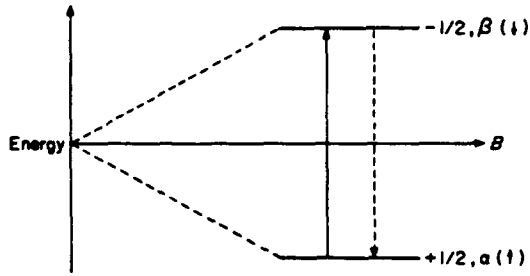

FIG. 3. Energy level for a nucleus with $I = \frac{1}{2}$ in a magnetic field.[4] (Reproduced by permission of Wiley, New York.)

the same at the NMR state, there would be no net absorption of energy from the radio-frequency (rf) radiation to the nuclei if the population of the nuclei in the two states were equal. Therefore, no NMR signal would be obtained.

However, in the thermal equilibrium state, the population of the nuclei in the lower energy level (N^-) is slightly in excess of that in the upper energy level (N^+) according to the Boltzmann equation [Eq. (12)],

$$N^-/N^+ = \exp(-\Delta E/T) \simeq 1 - \Delta E/\kappa T = 1 - 2\mu B_0/\kappa T \qquad (12)$$

where κ is Boltzmann constant and T is the absolute temperature. In general, the energy difference E is in the order of 10^{-2} cal/mol at a magnetic field in the range of 14,000–60,000 gauss. Consequently, the excess population of the nuclei in the lower energy level is in the order of 1 in 10^5 at 25°. This slight excess in the population of the nuclei in the lower energy level gives rise to a resultant magnetization vector $\mathbf{M}_0$ along the direction of B_0, i.e., z-axis in the stationary frame of reference, as shown in Fig. 4.

Relaxation Time

A finite period of time is required for the Boltzmann distribution to be established when an assembly of identical nuclei is placed in a strong constant magnetic field B_0. The nuclei undergo thermal motions and interact with their surroundings (lattice), including the magnetic field B_0.

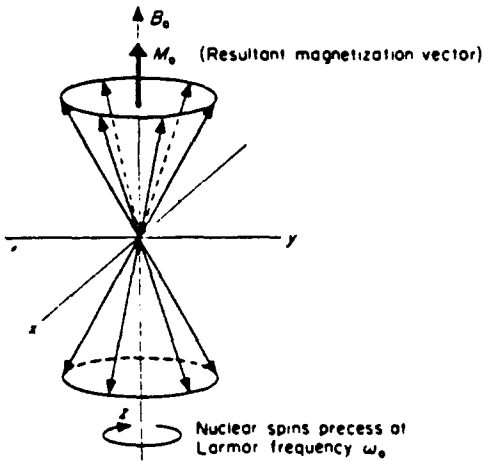

FIG. 4. Motion of nuclei with $I = \frac{1}{2}$ in a magnetic field.[4] (Reproduced by permission of Wiley, New York.)

This interaction involves energy transfer between the spin system and the lattice, resulting in transitions of the nuclei between allowed energy levels. This process is called spin–lattice or longitudinal relaxation and is a nonradiative first order process. The rate of the relaxation is inversely proportional to a relaxation time of T_1. The magnitude of T_1 depends on the physical state of the sample, the temperature, and the type of nucleus under observation. Nuclei of the same species with different chemical environments have different values of T_1. For liquids, T_1 values are generally in the range of 10^{-2}–10^2 sec for nuclei with $I = \frac{1}{2}$. Another relaxation process is the spin–spin or transverse relaxation, the rate of which is inversely proportional to a spin–spin relaxation time T_2. This process involves exchange of spin orientation between neighboring nuclei by interacting their magnetic moments. The process does not result in a change in the total energy of the system. The magnitude of T_2 is, in general, smaller than that of T_1, i.e., $T_1 \geq T_2$. The line width of the signal at midheight is equal to $1/2\pi T_2$ or $1/2\pi T_2^*$.

Motion of Magnetization Vector in Rotating Coordinate System

During NMR experiments, if the coordination system, i.e., the stationary frame of reference, is rotating about the z-axis at the angular velocity $\omega = 2\pi\nu$ of the rotating field B_1, then the path of the magnetization vector **M** subjected to the effects of magnetic fields B_0 and B_1 can be simplified. The rotating coordinate system is called the rotating frame of reference. The axes of the system are denoted as x', y', and z', as shown in Fig. 5, with the rotating unit vectors $\mathbf{i}'$, $\mathbf{j}'$, and $\mathbf{k}'$ for the components of **M** along x'-, y'-, and z'-axis, respectively.

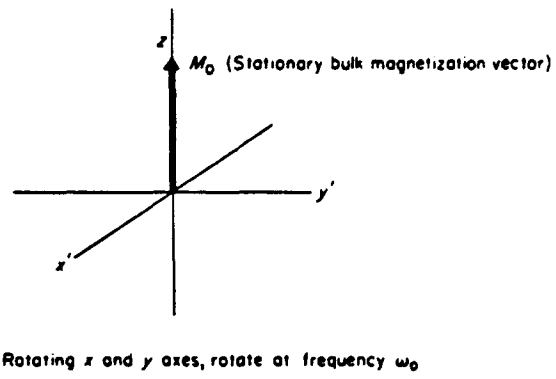

FIG. 5. Motion of nuclei with $I = \frac{1}{2}$ in a magnetic field rotating at the Larmor frequency ω_0 (the rotating frame reference system).[4] (Reproduced by permission of Wiley, New York.)

At NMR state, the magnetic moments of the nuclei with $I = \frac{1}{2}$ change their orientations with respect to the direction of the magnetic field B_0. For an assembly of nuclei with magnetic moment μ, the magnetization vector **M** is the resultant vector sum of the magnetic moments. The direction of **M** is now time dependent, and the change of **M** with time in the rotating frame of reference can be expressed by

$$\begin{aligned}(\partial \mathbf{M}/\partial t)_{\text{rot}} &= \gamma \mathbf{M}(B + \omega/\gamma) \\ &= \gamma \mathbf{M} B_{\text{eff}}\end{aligned} \tag{13}$$

where B is the total magnetic field resulting from the constant magnetic field B_0 and the rf field B_1, i.e., $B = B_0\mathbf{k}' + B_1\mathbf{i}'$, and B_{eff} is the effective magnetic field in the rotating frame of reference, defined by equation

$$\begin{aligned}B_{\text{eff}} &= (B + \omega/\gamma) \\ &= (B_0 + \omega/\gamma)\mathbf{k}' + B_1\mathbf{i}'\end{aligned} \tag{14}$$

Thus, the effect of rotating the coordinate system is to change the effective magnetic field by a term ω/γ resulting from the rotation.

Pulsed NMR Experiment in the Rotating Frame of Reference

In the absence of B_1, the vector **M** has its equilibrium value M_0 along the z'-axis. **M** is thus time-invariant in the rotating frame of reference, so that

$$(\partial \mathbf{M}/\partial t)_{\text{rot}} = \gamma \mathbf{M} B_{\text{eff}} = 0 \tag{15}$$

since $\mathbf{M} = M_0 \neq 0$ and $B_1\mathbf{i}' = 0$, combination of Eqs. (14) and (15) gives

$$B_{\text{eff}} = (B_0 + \omega/\gamma)\mathbf{k}' = 0 \tag{16}$$

Consequently, $(\omega/\gamma)\mathbf{k}' = -B_0\mathbf{k}'$. Thus, the rotational field ω/γ opposes $B_0\mathbf{k}'$ along the z'-axis in the rotating frame of reference as shown in Fig. 6. Equation (14) can then be rewritten

$$B_{\text{eff}} = (B_0 - \omega/\gamma)\mathbf{k}' + B_1\mathbf{i}' \tag{17}$$

Substituting Eq. (6) into Eq. (17), then

$$B_{\text{eff}} = 1/\gamma(\omega_0 - \omega)\mathbf{k}' + B_1\mathbf{i}' \tag{18}$$

If the frame of reference rotates about the z-axis at angular frequency ω matching the Larmor frequency ω_0 of the identical nuclei, then Eq. (18) becomes

$$B_{\text{eff}} = B_1\mathbf{i}' \tag{19}$$

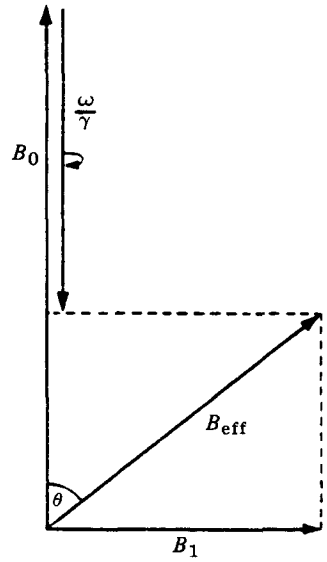

FIG. 6. The effective magnetic field in a rotating coordinate system.[1] (Reproduced by permission of Pergamon, Oxford, England.)

Substituting Eq. (19) into Eq. (13), then

$$(\partial \mathbf{M}/\partial t)_{rot} = \gamma \mathbf{M} B_1 \mathbf{i}' \tag{20}$$

This equation describes that, at NMR state, the magnetization vector **M** precesses about the field vector $B_1\mathbf{i}'$ of the radio-frequency. Since the coordinate system and the rf field B_1 are chosen to rotate about z'-axis at the same frequency, the direction of B_1 is always along the rotating x'-axis. Consequently, the angular precession frequency ω_1 of **M** about x'-axis also follows the Larmor equation [Eq. (6)].

$$\omega_1 = \gamma B_1 \tag{21}$$

Because angular frequency equals angular velocity, an application of a constant rf field B_1 for a short time $\mathbf{t_p}$ along the x'-axis causes the vector **M** to precess about the x'-axis from along the z'-axis toward the y'-axis by an angle θ, as shown in Fig. 7.

$$\theta = \omega_1 \mathbf{t_p} = \gamma B_1 \mathbf{t_p} \qquad \text{(radian)} \tag{22}$$

where $\mathbf{t_p}$ is pulse width (PW) and θ is flip angle. A rf pulse causing the vector **M** to precess $\theta°$ is called a $\theta°$ pulse, e.g., 30° pulse, 90° pulse, 180° pulse, etc.

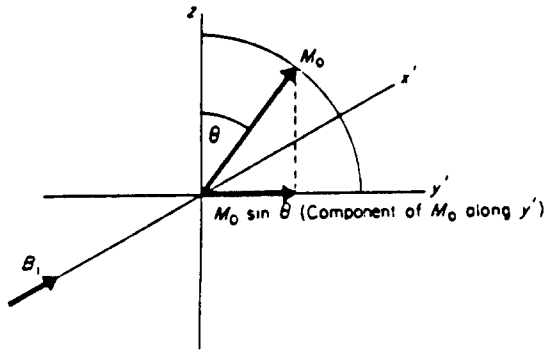

FIG. 7. Effect of a rf pulse with a frequency ω_0 for a time t (sec) on magnetization vector M_0.[4] (Reproduced by permission of Wiley, New York.)

Since the terms $(\omega_0 - \omega)\mathbf{k}'$ and $B_1\mathbf{i}'$ in Eq. (18) are components of vectors with respect to z'- and x'-axes in the rotating frame of reference, as shown in Fig. 6, the magnitude of the effective magnetic field B_{eff} is

$$|B_{\text{eff}}| = 1/\gamma[(\omega_0 - \omega)^2 + (\gamma B_1)^2]^{1/2} \tag{23}$$

If ω_0 is the angular precession frequency of all nuclei of the same nuclear species, and B_1 is chosen such that

$$\omega_0 - \omega \ll \gamma B_1 \tag{24}$$

then the term $(\omega_0 - \omega)$ can be neglected, and $B_{\text{eff}} \simeq B_1$. Since $(\omega_0 - \omega) = \Delta\omega = 2\pi\Delta\nu$, Eq. (24) becomes

$$2\pi\Delta\nu \ll \gamma B_1 \tag{25}$$

where $\Delta\nu$ is the spectral width (SW), i.e., the chemical shift range of the nuclei to be observed in the unit of Hz. Consequently, if B_1 is chosen large enough, the magnetization vector of all the nuclei having the Larmor frequency within the spectral width $\Delta\nu$ will precess about the x'-axis in the rotating frame of reference as a result of applying a rf field B_1 along the x'-axis.

In order to ensure that the magnetization vector of all the nuclei is rotated by the same angle, i.e., in phase, the pulse width $\mathbf{t_p}$ of the rf pulse applied must be considerably shorter than the relaxation times T_1 and T_2 of the nuclei, so that relaxation is negligible during the pulse. For a 90° pulse ($\theta = \pi/2$), the limiting condition for $\mathbf{t_p}$ can be estimated by substitution of $\theta = \pi/2$ and Eq. (22) into Eq. (25).

$$\mathbf{t}_{90} \ll 1/(4\Delta\nu) \qquad \text{sec} \tag{26}$$

In general, the pulse width for a 90° flip angle is in the range of 10–30 μsec for ^1H and ^{13}C nuclei. The magnitude of the pulse width depends on the magnetogyric ratio γ of the nucleus being observed, on the amplitude of the rf field [Eq. (22)] and on operational conditions of the NMR spectrometer. In practice, the frequency of rf pulse (carrier frequency) is adjusted in the middle of the spectral width. Compared to the single phase detection, where the carrier frequency is placed at one edge of the spectral width, i.e., slightly outside the sweep width, it has the advantage of a gain for the *S/N* ratio, by preventing the fold over of the base-line noise. In addition, it meets the requirement for a more uniform power level of the exciting rf pulse across the whole frequency range.

According to Eqs. (21) and (22), the application of a rf pulse of width $\mathbf{t_p}$ results in rotation of the magnetization vector M_0 along the z'-axis toward the y'-axis by an angle $\omega_1 \mathbf{t_p} = \theta$, as shown in Fig. 7. Consequently, immediately after the rf pulse, the component of M_0 along the y'-axis has the magnitude

$$\mathbf{M}_{y'} = M_0 \sin \omega_1 \mathbf{t_p} = M_0 \sin \theta \tag{27}$$

$\mathbf{M}_{y'}$ is also called the transverse magnetization. Thus, the signal induced in the receiver coil having its axis along the y' direction increases with $\mathbf{t_p}$, reaching a maximum for $\omega_1 \mathbf{t_p} = \pi/2$, a 90° pulse. For pulse width larger than 90°, the induced signal decreases and becomes zero for $\omega_1 \mathbf{t_p} = \pi$, a 180° pulse. In practice, a sample with a strong signal is used, and the pulse width is adjusted so that no signal is detected. One-half of this value is taken to be a 90° pulse.

Immediately after a θ° pulse, the transverse magnetization vector $\mathbf{M}_{y'}$ lies along the y'-axis. When the rf pulse is turned off, the vector $\mathbf{M}_{y'}$ decays exponentially to zero through spin–spin relaxation with the time constant $1/T_2$. Since the carrier frequency ω_1, i.e., the angular frequency of the rf pulse, is slightly off resonance, the vector $\mathbf{M}_{y'}$ rotates relative to the rotating frame of reference. At a time t after the pulse has been turned off, the vector $\mathbf{M}_{y'}$ has a phase shift of ωt relative to the y'-axis, where $\omega = (\omega_1 - \omega_0)$. Consequently, the vector $\mathbf{M}_{y'}$ does not precess with a constant phase shift of $\pi/2$ relative to the vector of B_1. Thus, the vectors $\mathbf{M}_{y'}$ and $\mathbf{B}_1'$ periodically rephase and dephase in the rotating frame of reference. As a result, a flux is induced in the receiver coil which alternates sign, and decays exponentially with time to zero when the Boltzmann equilibrium state is reestablished. The signal detected in the receiver is in the form of a beat pattern modulated by the difference in frequencies between the carrier frequency and the absorption frequency of the nuclei. In addition, the signal is also modulated with a frequency of J (Hz), where J is the coupling constant, if the nuclei being observed are spin coupled to another type of

nuclei species. A plot of the signal versus time as the nuclei return to the Boltzmann equilibrium state after the rf pulse is called the free-induced decay (FID) signal or time domain function $F(t)$. For a sample containing several nonidentical nuclei of the same nuclear species, the beat pattern is very complex, as shown in Fig. 8. The FID signal must be Fourier transformed to obtain frequency domain function $F(\omega)$ or spectrum.

For time average purposes, rf pulses are applied repeatedly at a constant interval with each FID being acquired, added, and stored in a time-averaging device. The time required for acquisition of the FID is called data acquisition time (AQ). The time between two pulses is referred to as the repetition time if it is a constant throughout the experiment; if not, it is called the pulse interval. The time between the end of data acquisition and the next pulse is called the pulse delay (RD), i.e., the difference between the repetition time and the data acquisition time. The number of the FID acquired during a NMR experiment is called the number of scans (NS). Accumulation of FIDs in a digital computer with concomitant noise averaging is known as the computer averaged transients (CAT) method. The signal/noise *(S/N)* ratio increases with the number of scans n according to Eq. (28).

$$(S/N)_n = (S/N)_1 (n)^{1/2} \tag{28}$$

For acquisition of FID data, each FID analog signal must be converted into digital form by an analog-to-digital computer (ADC). The FID is then recorded digitally as a series of several thousand data points, the number of which depends on the available data points N (memory capacity) of a digital computer. N is usually a power of 2, e.g., $2^{14} = 16{,}364$ (16K).

In order to obtain a true NMR spectrum after Fourier transformation, sufficient data points of each FID must be collected by the digital computer. The sampling time required to collect the sufficient data points depends on the spectral width $\Delta\nu$ (Hz). According to information theory,[25] two data points per cycle must be collected from each incoming signal. Thus, at least $2\Delta\nu$ data points per second must be collected for a spectrum with a spectral width $\Delta\nu$ (Hz). The maximal sweeping time per one data point, i.e., the dwell time (DW) t_{dw}, must then satisfy Eq. (29).

$$t_{dw} = (1/2\Delta) \qquad \text{sec/point} \tag{29}$$

For a spectral width of $\Delta\nu = 15{,}000$ Hz usually used in ^{13}C NMR spectra of lignin preparation at the NMR frequency for ^{13}C nuclei in the range of 60–63 MHz, the dwell time is 33.3 μsec.

[25] R. B. Blackman and J. W. Tudey, "The Measurement of Power Spectra." Dover, New York, 1958.

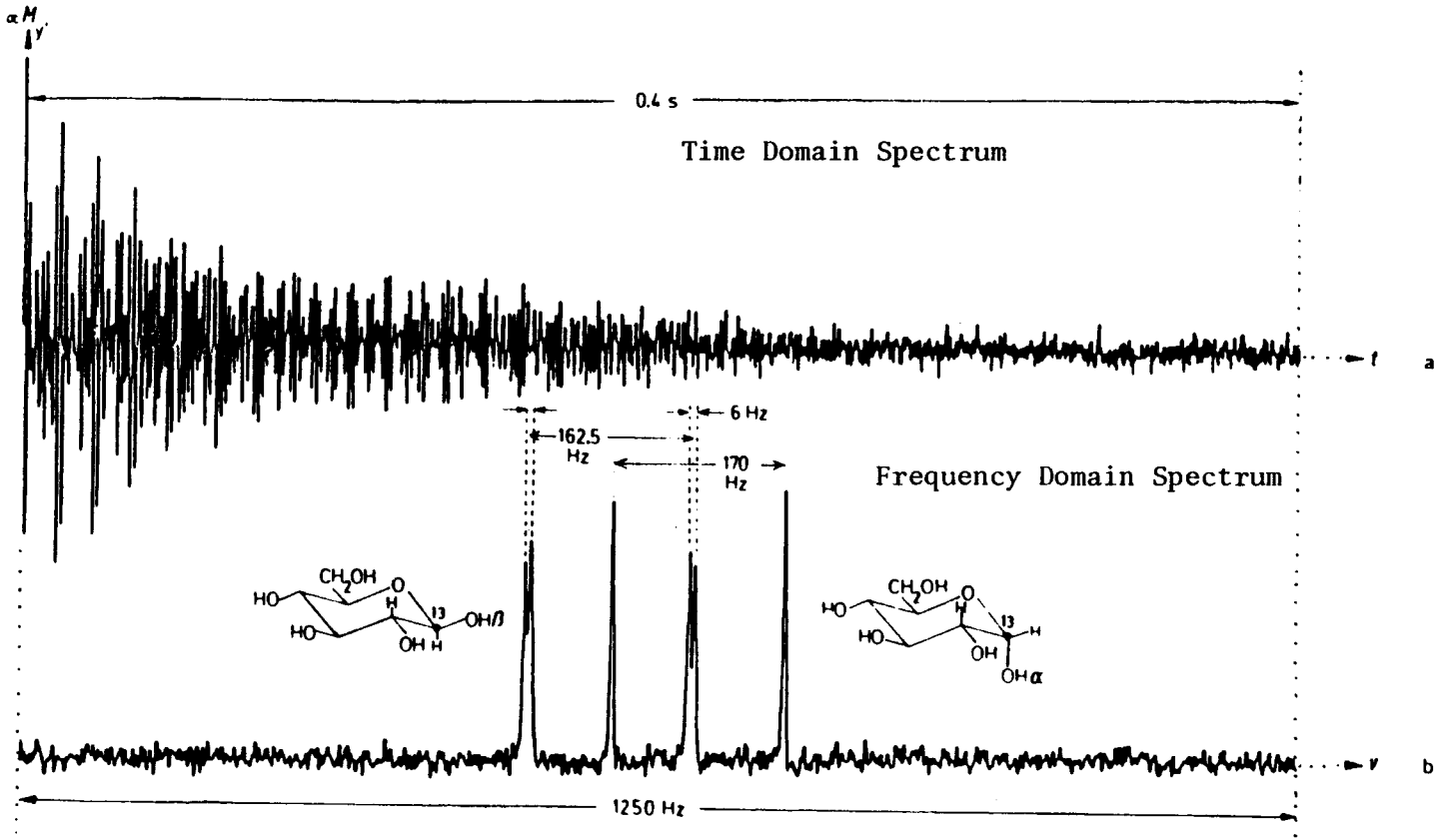

FIG. 8. (a) FID signal of mutarotated D-[1-^{13}C]glucose (60% ^{13}C) without proton decoupling. (b) Fourier transform of (a).[2] (Reproduced by permission of VCH Verlagsgesellschaft, Weinheim, Federal Republic of Germany.)

For a computer with the available data points N, the time required to fill up the memory capacity is

$$T_{aq} = Nt_{dw} = (N/2\Delta) \quad \text{sec} \tag{30}$$

where T_{aq} is the maximal data acquisition time (AQ) for recording a FID. For $\Delta\nu = 15{,}000$ Hz and $N = 16{,}394$ (16K), the maximal data acquisition is 0.55 sec. When several FIDs must be accumulated in order to improve the signal/noise ratio, T_{aq} is the minimal repetition time between two pulses.

Sample Preparations

Except for technical lignins, characterization of lignin by ^{1}H and ^{13}C NMR spectroscopy requires that the lignin should be isolated from plant tissues with minimal change in the structure. Milled wood lignin (MWL) is the best lignin preparation for this purpose (for the procedure for preparation of MWL from plant tissues, see chapter [14] in this volume). It must be mentioned that MWLs usually contain up to about 5% of carbohydrates, mainly hemicelluloses, and a small amount of fatty acids as contaminants. Since signals for ^{1}H and ^{13}C nuclei of these contaminants, particularly of carbohydrates, would appear at the aliphatic region of ^{1}H and ^{13}C NMR spectra of lignin, respectively, the contaminants should be removed from MWLs during purification as much as possible (for the procedure for purification of MWL, see chapter [14] in this volume). Technical lignins also need purification before using these lignins for the characterization. In order to ensure the purity of the lignin preparation, the following analyses of the lignin should be conducted before using it for the structural analysis by ^{1}H and ^{13}C NMR spectroscopy: (1) elemental analysis including methoxyl content, (2) moisture content (for the procedure, see chapter [14] in this volume), (3) total lignin content (for the procedure, see chapter [14] in this volume), and (4) carbohydrate analysis by a suitable procedure either according to Borchardt and Piper[26] or Fengel *et al.*[27] If the carbohydrate content of a lignin preparation is appreciably more than 5% or a carbohydrate-free lignin preparation is required, the lignin preparation should be purified again according to the procedure of Lundquist *et al.*[28]

[26] L. G. Borchardt and C. V. Piper, *Tappi* **53**, 257 (1970).
[27] D. Fengel, G. Wegener, A. Heizmann, and M. Przklenk, *Holzforschung* **31**, 65 (1977).
[28] K. Lundquist, B. Ohlsson, and R. Simonson, *Sven. Papperstidn.* **80**, 143 (1977).

Characterization of Lignin by ^1H NMR Spectroscopy

Reagents

Acetic anhydride
Pyridine
Deuterochloroform ($CDCl_3$) containing 1% tetramethylsiline (TMS)

Preparation of Acetylated Lignin

To a solution of 400-mg lignin preparation, either MWL or technical lignin, in 6 ml of pyridine is added 3 ml of acetic anhydrate. The mixture is kept at room temperature for 48 hr. Centrifuge the reaction mixture to remove insoluble materials, if any. The reaction mixture is then poured into about 40 g of crushed ice in a 100-ml beaker to precipitate acetylated lignin. Adjust the resulting mixture to pH 3 by adding concentrated HCl dropwise, and keep the mixture overnight at room temperature. The precipitate is centrifuged off, is stirred with about 30 ml of distilled water in the centrifuge bottle for about 30 min, and is again centrifuged off. The precipitate is washed once more and then is suspended in about 20 ml of distilled water and is freeze-dried. The final product is dried in a drying pistol over P_2O_5 at 50° under vacuum for 48 hr. The product should be free from pyridine and acetic acid.

^1H NMR Spectrum of Acetylated Lignin

Weigh about 35 mg of dried acetylated lignin. Dissolve the specimen in 0.5 ml of $CDCl_3$ containing 1% TMS (v/v), TMS being the internal reference. The concentration of the sample is about 7% (w/v). Filter off insoluble materials, if any, with beaker filtering (filter disk, 10 mm, i.d.; porosity, 25–50 μm). The solution is transferred to a 5-mm (o.d.) sample tube. The sample solution is then placed in the probe of a ^1H NMR spectrometer operating at 90, 100, 200 or 250 MHz, preferably one of the latter two, and the spectrum is recorded at 25° (298°K) or room temperature. When Fourier transformation (FT) mode is used with ^2H nucleus in $CDCl_3$ as an internal lock for the spectrometer field frequency, then a ^1H NMR spectrum of the acetylated lignin is obtained with pulse width corresponding to flip angle in the range of 60–90°, data acquisition time of about 2–3 sec, pulse delay of 0–2 sec, and the number of scans being about 20. The selection of the operational parameter depends on the nature of ^1H NMR spectrometer. Figure 9 shows a ^1H NMR spectrum of acetylated MWL prepared from sapwood of Zhong-Yang Mu *(Bischofia polycarpa)* recorded at $\nu\ ^1H = 250$ MHz with a Bruker WM 250 NMR spectrometer.[29]

[29] D. Robert, D. Tai, and C.-L. Chen, *Holzforschung*, submitted for publication.

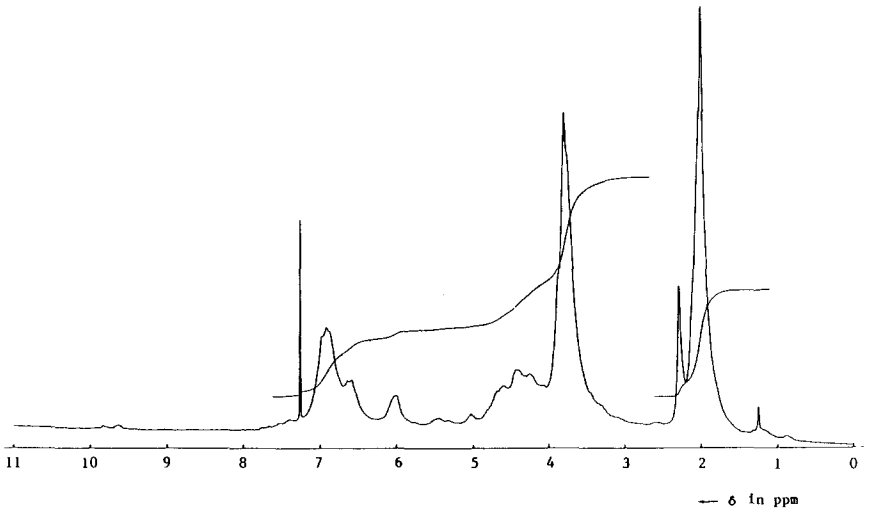

FIG. 9. ^{1}H NMR spectrum of acetylated milled wood lignin (acetylated MWL) from wood of *B. polycarpa*.

The spectrum is obtained in $CDCl_3$ at 25° in the FT mode with the pulse width 10.5 sec (90° pulse), the data acquisition time about 2.7 sec without a pulse delay, and the number of scans being 16.

Considerable line broadening would be observed in a NMR spectrum if solid materials and paramagnetic and/or ferromagnetic impurities are present in the sample solution. In addition to removal of any insoluble materials from the sample solution, care must be taken to ensure that these impurities are eliminated from the sample solution. For example, after a sample tube is cleaned with a cleaning solution, the tube must be washed thoroughly with distilled water until the tube is free from Cr(III), Cr(II), and other heavy metal ions, then must be rinsed thoroughly with acetone, and finally with carbon tetrachloride. The tube is then dried in a drying pistol or an oven under vacuum at 50° for at least 2 hr to remove any trace of the solvents.

Interpretation of ^{1}H NMR Spectra of Acetylated Lignins

As shown in Fig. 9, ^{1}H NMR spectra of acetylated lignins are not only complex, but are also not well resolved. This is also true for ^{1}H NMR of underivatized lignins using DMSO-d_6 as a solvent. These disadvantages are attributable to the polymeric and complex nature of lignin in terms of the chemical structure, in addition to the rather narrow ^{1}H chemical shift range. The ^{1}H nuclei in lignins present in similar, but not identical, chemical environments give rise to intensive overlap of signals in the spectra. In

addition, the overlap is enhanced by the multiplication of the signals due to J scalar couplings. The presence of carbohydrates in lignin preparations would make the spectra even more complex. Thus, interpretation of the spectra entirely depends on the spectral data obtained from the ^1H NMR spectroscopic study of the lignin model compounds. Table I summarizes chemical shifts of ^1H nuclei present in the major substructures of acetylated lignins and possible contaminants.

TABLE I

CHEMICAL SHIFTS OF ^1H NUCLEI IN SUBSTRUCTURES OF ACETYLATED LIGNINS AND POSSIBLE CONTAMINANTS

Spectral region	Chemical shift range of (δ in ppm)	Types of ^1H nucleus
1	9.00–12.00	**Strongly Deshielded Region**
	10.00–12.00	Hydrogens in carboxylic acid groups in acetylated substructur and in *O*-alkylated uronic acid moieties in acetylated pentosar and fatty acids (minor contaminants)
	9.00–10.00	Hydrogens in aldehyde groups in cinnamaldehyde moieties in ac tylated substructures (minor components)
2	6.25– 7.90	**Aromatic Region**
	7.80– 7.90	Aromatic hydrogens ortho to carbonyl group in acetylated an 4-*O*-alkylated *p*-hydroxyphenylpropane moieties with α—C= in acetylated substructures
	7.23– 7.80	Aromatic hydrogens ortho to —C=O group in acetylated and 4-(alkylated guaiacylpropane moieties with α—C=O group in ac tylated substructures. Also, hydrogens on C-α of cinnamaldehyc and cinnamic acid moieties in acetylated substructures (min components)
	7.23– 7.30	Aromatic hydrogens ortho to carboxyl group in acetylated an 4-*O*-alkylated syringylpropane moieties with α—C=O group i acetylated substructures
	6.80– 7.20	Aromatic hydrogens in acetylated and 4-*O*-alkylated *p*-hydrox phenylpropane moieties of acetylated substructures
	6.35– 7.25	Aromatic hydrogens of acetylated and 4-*O*-alkylated guaiacylpr pane moieties of acetylated substructures. Also, hydrogens on C- of cinnamaldehyde and cinnamic acid moieties in acetylate substructures (minor components)
	6.25– 6.70	Aromatic hydrogens in acetylated and 4-*O*-alkylated syringylpr pane moieties of acetylated substructures. Also, hydrogens c C-α of arylvinylene group in cinnamyl alcohol moieties of acet lated substructures (minor components)
3	5.75– 6.25	**Noncyclic Benzylic Region**
	6.10– 6.25	Hydrogens on C-β of arylvinylene group in cinnamyl alcohol moi ties of acetylated substructures (minor components)
	5.75– 6.25	Hydrogens on C-α of acetylated β-*O*-4, β-1, and arylglycerol sul structures (the latter two, minor components)

TABLE I *(continued)*

Spectral region	Chemical shift range of (δ in ppm)	Types of ^{1}H nucleus
4	5.20– 5.75	**Cyclic Benzylic Region**
	5.20– 5.75	Hydrogens on C-α in moiety A of acetylated β-5 and α-*O*-4 substructures
	5.20– 5.50	Hydrogens on C-3 of acetylated pentosans (minor contaminants)
5	2.50– 5.20	**Methoxyl and Major Aliphatic Region**
	4.50– 5.20	Hydrogens on C-β of acetylated β-*O*-4 substructures, on C-γ of cinnamyl alcohol acetate moieties in acetylated substructures, and on C-α of acetylated β–β substructures (the latter two, minor components). Also, hydrogens in C-1 and C-2 of acetylated pentosans and on C-2 and/or C-3 of acetylated hexosans (both minor contaminants)
	3.95– 4.50	Hydrogens on C-γ of acetylated β-*O*-4, β-5, β-1, and equatorial hydrogens on C-γ of β–β substructures (the latter two, minor components). Also, hydrogens on C-4 of acetylated pentosans and on C-1, C-4, and C-6 of acetylated hexosans (both minor contaminants)
	3.55– 3.95	Methoxyl hydrogens in aromatic moieties of acetylated substructures, hydrogens on C-β of β-5 and axial hydrogens on C-γ of β–β substructures. Also, hydrogens on C-5 of acetylated pentosans and hexosans (minor contaminants)
	2.50– 3.55	Hydrogens on C-β in acetylated β-1 and β–β substructures (both minor components). Also, methoxyl hydrogen in acetylated pentosans, hydrogens on —CH_2COOH moieties of fatty acids (all three, minor contaminants)
6	2.20– 2.50	**Aromatic Acetoxyl Region**
	2.20– 2.50	Acetoxyl hydrogens in aromatic moieties of acetylated substructures, except for acetylated 5–5 substructures
7	1.60– 2.20	**Aliphatic Acetoxyl Region**
	1.60– 2.20	Acetoxyl hydrogens in aliphatic moieties of acetylated substructures and in aromatic moieties of acetylated 5–5 substructures
8	0.75– 1.60	**Nonoxygenated Aliphatic Region**
	1.10– 1.60	Hydrogens on —CH_2—CH_2—CH_2— and —$(CH_2)_2$—CH— moieties of fatty acids and similar aliphatic compounds (all minor contaminants)
	0.75– 1.10	Hydrogens on terminal CH_3— groups in fatty acids and similar aliphatic compounds (all minor contaminants)

The spectrum of acetylated MWL of *B. polycarpa* is analyzed according to Table I.[29] In addition, the major substructure and functional groups are determined semiquantitatively. The results are given in Table II. The lignin contains about 5.6% of carbohydrates, of which about two-thirds are pentosans and the remainder hexosans. Moreover, the lignin has a C_9 unit

TABLE II

RESULTS FROM ^{1}H NMR SPECTRUM OF ACETYLATED MILLED WOOD LIGNIN (MWL) PREPARED FROM SAPWOOD OF ZHONG-YANG MU (*Bischofia polycarpa*)[a]

Chemical shift range (δ in ppm)	Integral	Number of hydrogens	Number of hydrogens after carbohydrate correction	Type of hydrogens
9.58–9.86	Negligible	0.02	0.02	C*H*O in Ar—CH═CH—CHO
7.23–7.90	2.1	0.14	0.14	Ar—H in Ar—COR
6.25–7.23	35.2	2.34	2.34	Ar—H in Ar—R
				H-α in Ar—CH═CH—CHO
				H-β in Ar—CH═CH—CHO
				H-α in Ar—CH═CH—CH_2OAc
5.75–6.25	6.0	0.40	0.40	H-α with α-O-Ac in β-*O*-4 and β-1
				H-β in Ar—CH═CH—CH_2OAc
5.20–5.75	2.8	0.19	0.14	H-α with α-O-Ac in β-5 (0.09/C_9)
				H-α with α-O-Ac in β-*O*-4 and β-1 (0.05/C_9)
4.50–5.20	11.2	0.74	0.58	H-β in β-*O*-4
				H-γ in Ar—CH═CH—CH_2OAc
				H-α in β–β
3.95–4.50	26.5	1.76	1.60	H-γ in β-*O*-4, β-5, β-1,
			(0.80)	and β–β
3.55–3.95	55.0	3.65	3.52	Ar—O—CH_3, (3.39/C_9)
				H-β in β-5 (0.09/C_9)
				H-γ in β–β (0.04/C_9)
2.50–3.55	8.4	0.56	0.56	H-β in β-1, β–β, and others
2.20–2.50	9.0	0.60	0.60	H in Ar—OAc except for 5–5 unit
1.50–2.20	63.8	4.23	3.69	H in Aliph—OAc and Ar—OAc in 5–5 units
1.10–1.50	0.4	0.03	0.03	—
0.75–1.10	+		+	—

[a] From Robert *et al.*[29]

formula $C_9H_{6.59}O_2(H_2O)_{0.89}(OCH_3)_{1.13}$ (C_9 unit weight: 197.83) after correction of the carbohydrate content (for analytical data, see chapter [14], Table I, in this volume). This means that one C_9 unit weight (g) of the lignin is associated with about 11.74 g of carbohydrates. Assuming that the mean monomeric unit for pentosans and hexosans are $C_{5.6}H_{8.8}O_{4.4}$ (unit weight: 146.53) and $C_6H_{10.2}O_{5.1}$ (unit weight: 162.94), respectively, then the carbohydrates consist of about 7.83 g (0.053 mol) of pentosans and about 3.91 g (0.024 mol) of hexosans. As shown in Table I, the aromatic methoxyl region (3.55–3.95 ppm) of ^{1}H NMR spectra of lignins also contains signals for ^{1}H nuclei on C-β of acetylated phenylconmaran (β-5) substructures, axial ^{1}H nuclei on C-γ of pinoresinol-type (β–β) substructures, and ^{1}H nuclei on C-5 of acetylated pentosans and hexosans. The C_9 unit formula of the MWL from *B. polycarpa* indicates that the lignin is rather close to MWLs from woods of gymnosperms. The lignin of this type usually contains about 0.09–0.12 and 0.02 U/C_9 unit of β-5 and β–β substructures,[24] respectively, in addition to up to about 5% of carbohydrates. Thus, the area of signals in the aromatic methoxyl region (3.55–3.95 ppm) of the spectrum should correspond to about 3.65 ^{1}H nuclei ($=3 \times 1.13 + 0.09 + 2 \times 0.02 + 2 \times 0.053 + 0.024$). Since the integral for the area is 55, the integral for one ^{1}H nucleus corresponds to 15.07. The integrals of the other chemical shift ranges are divided by the integral for one ^{1}H nucleus, i.e., 15.07, with a correction due to carbohydrates and other contaminants, if any, to estimate the number of ^{1}H nuclei due to the acetylated MWL in these ranges.

The total aromatic hydrogens in the acetylated MWL from *B. polycarpa* is estimated to be about 2.39–2.42/C_9 units from the aromatic region (6.25–7.90 ppm) of the spectra, taking account of the possible presence of Ar—CH=CH—CHO and Ar—CH=CH—CH_2OH, each about 0.02–0.03 U/C_9 unit in the lignin. The aromatic region also contains signals for ^{1}H nuclei on C—α and C—β of Ar—CH=CH—CHO and on C—α of Ar—CH=CH—CH_2—OAc. Since the MWL has 1.13 OCH_3 groups/C_9 unit, the lignin could consist of guaiacylpropane and syringylpropane units in the approximate molar ratio of 0.87:0.13. If the lignin did not contain any condensed aromatic moiety, the total aromatic hydrogens of the lignin would be 2.87/C_9 unit ($=3 \times 0.87 + 2 \times 0.13$). The deficiency in the total aromatic hydrogens between the assumed and estimated values, about 0.45–0.48/C_9 unit ($=2.87 - 2.42$ or 2.39), is the degree of condensation involving aromatic moieties of the lignin. The number of aromatic acetoxyl groups, excluding those of biphenyl (5–5) substructures, are estimated to be about 0.20/C_9 unit from the aromatic acetoxyl region (range, 2.20–2.50 ppm), while the number of aliphatic acetoxyl groups, including those of 5–5 substructures, is determined to be

1.23/C_9 unit. An inspection of the other regions of the spectrum indicates that the acetylated MWL contains a total of about 1.18/C_9 unit aliphatic acetoxyl groups, about 0.38/C_9 unit on C—α (range, δ 5.75–6.25 ppm), about 0.02/C_9 unit of C—γ of Ar—CH=CH—CH_2—OAc (range, δ 4.50–5.20 ppm), and about 0.78/C_9 unit of C—γ of β—*O*—4, β—5, and β—1 substructures (range, δ 3.95–4.50 ppm). Thus, the number of aromatic acetoxyl groups in 5–5 substructures is estimated to be about 0.05/C_9 unit (= 1.23 − 1.18). Therefore, the aliphatic and phenolic hydroxyl contents in the MWL are determined to be about 1.18/C_9 unit and 0.25/C_9 unit, respectively. The spectrum also indicates that the lignin contains about 0.50 U/C_9 unit of β—*O*—4 substructures (range, δ 4.50–5.20 ppm), and, probably, 0.08–0.09 and 0.05–0.06 U/C_9 unit of β—5 and α—*O*—4 substructures, respectively. However, the quantity of other substructures cannot be estimated even in first approximation, mainly, because of line broadening caused by the overlap of signals.

Characterization of Lignin by ^{13}C NMR Spectroscopy

Reagents

Hexadeuterodimethyl sulfoxide (DMSO-d_6)
Hexadeuteroacetone (acetone-d_6)–deuterium oxide (D_2O) (9 : 1, v/v)

Samples and Solvents

Purified MWLs, technical lignins, and acetylated lignin preparations are usually used as samples for obtaining ^{13}C NMR spectra (for purification of lignin preparation, see *Sample preparation* in this chapter, and for the procedure for the preparation of acetylated lignin, see *Preparation of Acetylated Lignin*). Either DMSO-d_6 or acetone-d_6–D_2O (9 : 1, v/v) is used as solvent for MWLs and technical lignins. Usually, DMSO-d_6 is employed as the solvent for these lignin preparations because of greater solubility. For acetylated lignins, acetone-d_6–D_20 (9 : 1, v/v) is used as the solvent.

Preparation of Sample Solution

Weigh about 300–400 mg of dried lignin preparation. Dissolve the specimen in 2 ml of suitable solvent, TMS being the internal reference. Filter off insoluble materials, if any, with a beaker–filter (filter disk, 10 mm, i.d.; porosity, 25–50 μm). The concentration of the specimen is about 15–20% (w/v). The solution is transferred into a 10-mm (o.d.) tube, preparatory to running the ^{13}C NMR spectrum of the lignin. The sample tube must be thoroughly cleaned (for details, see *^1H NMR Spectrum of Acetylated Lignin*).

Routine ^{13}C NMR Spectra

^{13}C NMR spectrum of a lignin preparation in a suitable solvent is usually obtained with a ^{13}C NMR spectrometer operating in a pulse Fourier transform (FT) mode at NMR frequency for ^{13}C nucleus (ν ^{13}C) more than 50 MHz. JEOL FX60 and CX100 NMR spectrometers operate at ν ^{13}C of 14.9 and 100.4 MHz, respectively, while Bruker MW 200, 250, and 400 NMR spectrometers operate at ν ^{13}C of 50.3, 62.9, and 100.4 MHz, respectively. A sample solution of a lignin preparation is placed in the probe of a NMR spectrometer, and ^{2}H nucleus of the solvent, i.e., the ^{2}H nucleus in either DMSO-d_6 or acetone-d_6 is used as the internal lock for the spectrometer field frequency. Routine ^{13}C NMR spectrum of the lignin preparation is then obtained, in general, at 25–50° with a pulse width corresponding to a flip angle in the range of 30–60°, acquisition time about 0.5–1.0 sec, a pulse delay about 0.5–2 sec, and a number of scans about 10,000–20,000. Tetramethylsilane (TMS) is usually used as chemical shift reference, i.e., chemical shifts of signals are expressed in δ values (δ in ppm). The optimal parameters for operation of a spectrometer are determined on the basis of experimental data and the nature of the spectrometer. The broadband noise proton decoupler is turned on during the experiment as shown in Fig. 10.

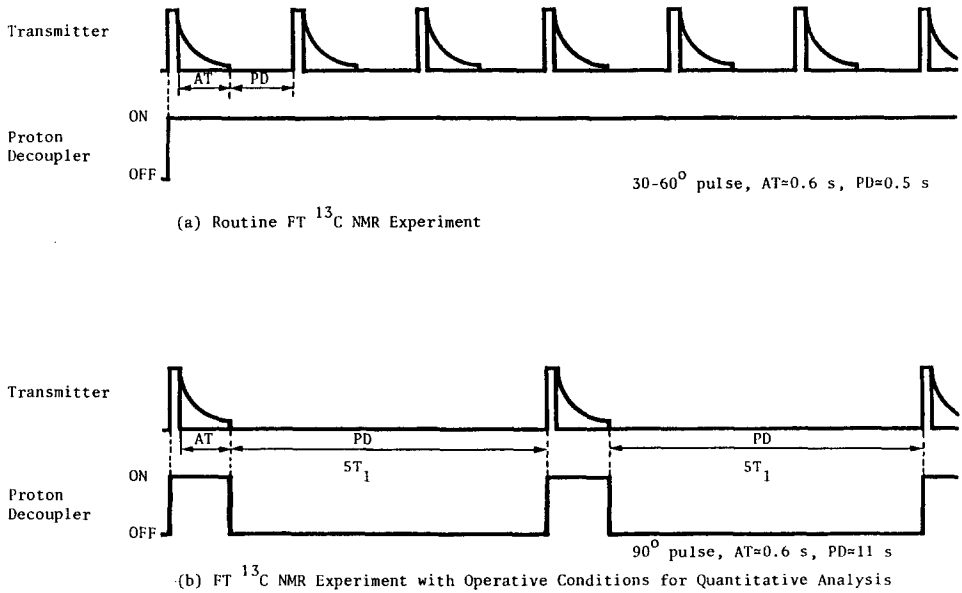

FIG. 10. Routine and inverse gated decoupled FT ^{13}C NMR experiments.

Figure 11 shows a ^{13}C NMR spectrum of MWL from wood of birch *(Betula papyrifera)* recorded at $\nu\ ^{13}C = 14.9$ MHz with a JEOL FX 60 NMR spectrometer. The spectrum is obtained in DMSO-d_6 at 50° with the pulse width 20 μsec (60° pulse), the data acquisition time about 1 sec, the pulse repetition time 2 sec, and the number of scans about 20,000. The broadband noise proton decoupler is applied during the operation. Figure 12 shows a ^{13}C NMR spectrum of MWL from wood of birch *(Betula verrucosa)* recorded at $\nu\ ^{13}C = 62.9$ MHz with a Bruker WM 250 NMR spectrometer. The spectrum is obtained in DMSO-d_6 at 50° with the pulse width 22 sec (90° pulse), the acquisition time 0.573 sec, the pulse delay 0.527 sec, and the number of scans being 37,000. The broadband noise proton decoupler is applied during the experiment.

A comparison of the spectrum of birch MWLs reveals that the spectrum recorded on a Bruker WM 250 spectrometer ($\nu\ ^{13}C = 62.9$ MHz) has a better resolution and more stable baseline, in fact a better *S/N* ratio than the spectrum recorded on a JEOL FX 60 spectrometer ($\nu\ ^{13}C = 14.9$ MHz). The resolution depends, in fact increases, on the instrument frequency and on the memory size of the analog-to-digital computer (ADC), respectively, 16,384 versus 8,192 data points for the Bruker and JEOL spectrometers. The signal-to-noise ratio, which defines the sensitivity, depends on B_0 to a power of 3/2, that means, increases by a factor of about eight, on going from 60 MHz (1.4092 *T*) to 250 MHz (5.872 *T*). This clearly demonstrates advantages of operating at a higher field.

Proton decoupling increases the intensity of ^{13}C signals because the intensity of all multiple lines in a ^{1}H- and ^{13}C-coupled spectrum are accumulated in one singlet signal in the decoupled spectrum. However, the intensity of a ^{13}C signal for CH group increases more than twice on proton decoupling. This additional sensitivity enhancement is known as the nuclear Overhauser effect (NOE). The maximal NOE enhancement factor $F_A(X)$ for the *A* signal for *AX* group in a *X* nuclei decoupling experiments depends on the magnetogyric ratios of *A* and *X*.[30]

$$f_A(X) = \gamma_X/2\gamma_A \tag{31}$$

Since γ for $^{13}C = 6{,}726$ rad sec^{-1} gauss^{-1} and γ for $^{1}H = 26{,}752$ rad sec^{-1} gauss^{-1}, the maximal NOE enhancement factor for CH groups is about 1.99. For CH_3 and CH_2 groups, the maximal NOE enhancement increases proportional to the number of attached protons. In contrast, quaternary carbons do not undergo the NOE enhancement. Thus, this is one reason why the area of ^{13}C signals in a proton decoupled ^{13}C NMR spectrum is not proportional to the number of the corresponding ^{13}C nuclei.

[30] J. H. Noggle and R. E. Schirmer, "The Nuclear Overhauser Effect: Chemical Applications." Academic Press, New York, 1971.

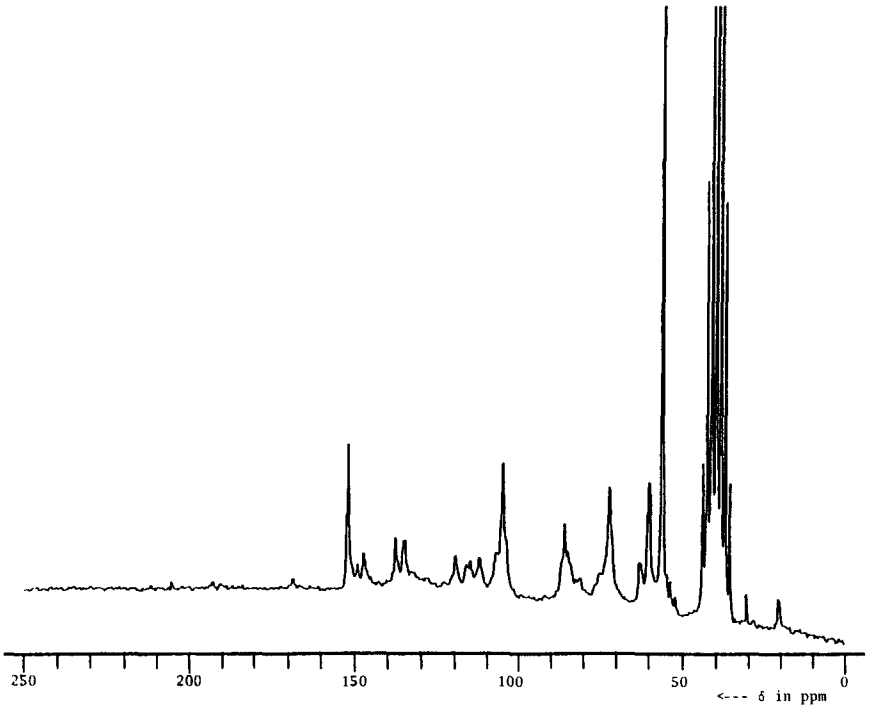

FIG. 11. Routine ^{13}C NMR spectrum of MWL from wood of birch *(B. papyrifera)*.

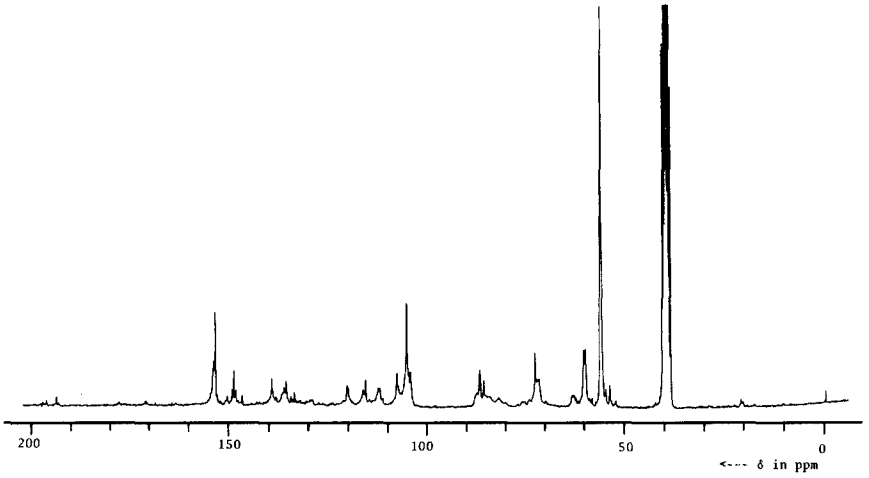

FIG. 12. Routine ^{13}C NMR spectrum of MWL from wood of birch *(B. verrucosa)*.

Quantitative ^{13}C NMR Spectra: Inverse Gated Decoupling Sequence

In order to obtain a quantitative ^{13}C NMR spectrum of a lignin preparation, the following factors must be considered: (1) pulse width, (2) time required to reestablish the Boltzmann equilibrium state after the rf pulse, (3) elimination of the NOE sensitivity enhancement due to proton decoupling, and (4) the number of scans in order to obtain a reasonable signal-to-noise ratio.

As described previously, NMR spectrometers only detect signals along the y'-axis in the rotating frame of reference. This requires that a 90° pulse should be applied, since the pulse produces the maximal transverse magnetization vector $\mathbf{M}_{y'}$ along the y'-axis immediately after the pulse according to Eq. (27), i.e., $\mathbf{M}_{y'(0)} = M_0 \sin 90° = M_0$, $\mathbf{M}_{x'(0)} = 0$, $\mathbf{M}_{z'(0)} = M_0 \cos 90° = 0$. After the 90° pulse, the magnetization vectors relax back to the Boltzmann equilibrium state via first order spin–lattice and spin–spin relaxation processes along the z'-axis and the $x'y'$ plane with time constants $1/T_1$ and $1/T_2$, respectively. Without considering the spin–spin relaxation, the signal detected along the y'-axis decays away via the spin–lattice relaxation according to

$$\mathbf{M}_{y'(t)} = \mathbf{M}_{y'(0)} \exp(-t/T_1) = M_0 \exp(-t/T_1) \tag{32}$$

where $\mathbf{M}_{y'(0)}$ and $\mathbf{M}_{y'(t)}$ are the magnetization vector along the y'-axis at time 0 sec and t sec after the application of a 90° pulse. The magnitude of $\mathbf{M}_{y'(0)}$corresponds to that of M_0 along the z'-axis at the Boltzmann equilibrium state. After a time T_1 (sec), the vector $\mathbf{M}_{y'(0)}$decays to $\mathbf{M}_{y'(T_1)} = 0.3679\, M_0$; and after a time $5T_1$ (sec), it decays to $\mathbf{M}_{y'(5T_1)} = 0.0067\, M_0$, essentially zero. At the same time, the vector $\mathbf{M}_{y'(0)}$ also decays via the spin–spin relaxation according to

$$\mathbf{M}_{y'(t)} = \mathbf{M}_{y'(0)} \exp(-t/T_2) = M_0 \exp(-t/T_2) \tag{33}$$

The spin–spin relaxation may be accelerated due to inhomogeneities in the magnetic field, so that $(1/T_2^*)_{\text{inhomo}} \leq 1/T_2 \leq 1/T_1$. If $T_1 \simeq T_2^*$, the pulse can be repeated after a pulse delay of about $3T_2^*$ without loss in signal intensity. However, if $T_1 \ll T_2^*$, a pulse delay of about $5T_1$ is required to reestablish the Boltzmann equilibrium state.

The elimination of the NOE sensitivity enhancement can be accomplished by application of the inverse gated proton decoupling sequence. As shown in Fig. 10,[31] the proton decoupler is turned off prior to the 90° pulse so that, when the pulse is applied, the magnetic moments of the ^{13}C nuclei are at the Boltzmann equilibrium state. The decoupler is turned on at the

[31] D. Robert, *Proc. Can. Wood Chem. Symp. 1982* p. 63 (1982).

same time the pulse is applied. Since the sample undergoes proton decoupling during data acquisition time, a full spectrum with no signal enhancement is obtained. The proton decoupling during data acquisition time perturbs the equilibrium state of the system. Consequently, when the decoupler is turned off immediately after the data acquisition, the system is no longer at the Boltzmann equilibrium state. In order to reestablish the equilibrium state, a pulse delay of $5T_1$ sec is required.

The T_1 of all signals in the ^{13}C NMR spectrum of MWL from birch wood *(B. verrucosa)* has been determined by the inversion recovery method.[32-33] Among the T_1s observed for the signals investigated, the longest T_1 is chosen as the standard to estimate the pulse delay required. At operating frequency ν ^{13}C = 50.32 and 62.29 MHz, the optimal pulse delay is determined to be about 10 sec for MWLs and about 12 sec for acetylated lignin preparation.[31,33] Thus, the operational condition to obtain quantitative ^{13}C NMR spectra of lignin preparation is determined to be the inverse gated decoupling (IGD) sequence with the 90° pulse, the pulse delay about 10 sec, and the number of scans about 10,000. For acetylated lignin preparation, the pulse delay is about 12 sec.[34,35] The quantitative nature of the ^{13}C NMR spectra thus obtained has been verified.[31,33] However, the spectra could still have an error of about ±5% with respect to the proportionality between the area under a signal and the number of the ^{13}C nuclei giving rise to the signal.

Figure 13 shows a quantitative ^{13}C NMR spectrum of MWL from wood of Zhong-Yang Mu *(B. polycarpa)* recorded at 50° in DMSO-d_6 with a Bruker WM 200 NMR spectrometer operating at ν ^{13}C = 50.32 MHz. The spectrum is obtained by the IGD sequence with the pulse width of 15 μsec (90° pulse), the data acquisition time of 0.7 sec, the pulse delay equal to 10 sec, and the number of scans being 9000. Figure 15d shows a quantitative ^{13}C NMR spectrum of MWL from wood of birch *(B. verrucosa)* recorded at the same experimental conditions for obtaining the spectrum of the MWL from *B. polycarpa.*

Distortionless Enhancement by Polarization Transfer (DEPT) Sequence

The DEPT sequence is a one-dimensional pulse sequence, which involves spin echo phenomenon, and allows separate observation of the ^{13}C NMR signals for the CH, CH_2, and CH_3 groups. In addition to clearly

[32] R. Freeman and H. D. W. Hill, *J. Chem. Phys.* **53,** 4103 (1971).
[33] D. Robert and D. Gagnaire, *Ekman Days, Int. Symp. Wood Pulp. Chem.* **1,** 86 (1981).
[34] D. Robert and G. Brurow, *Holzforschung* **38,** 85 (1984).
[35] D. Robert, M. Bardet, G. Gellerstedt, and E. L. Lindfords, *J. Wood Chem. Technol.* **4,** 239 (1984).

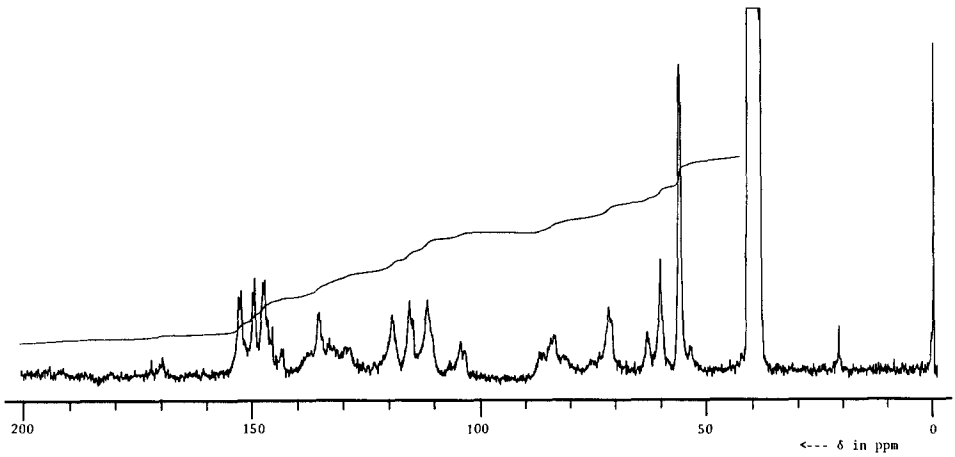

FIG. 13. Guantitative ^{13}C NMR spectrum of MWL from *B. polycarpa.*

revealing the multiplicity of the carbon atoms, there is a large signal intensity enhancement due to the polarization transfer. This polarization transfer relies on a spin population interchange between the more sensitive nucleus (^1H) and the less sensitive nucleus (^{13}C) to the benefit of the latter. As in the INEPT sequence,[36] the polarization transfer in the DEPT sequence is accomplished nonselectively through modulations of the transverse magnetization of the more sensitive nucleus (^1H) via its coupling to the less sensitive nucleus (^{13}C) by application of 180°x pulses in the ^1H and ^{13}C frequency regions, as indicated in the DEPT sequence scheme shown in Fig. 14.[22] The advantage of the DEPT sequence over the INEPT sequence is 2-fold, i.e., the DEPT sequence not only provides the same intensity enhancement for each line of a multiplet without phase distortion, but also is nearly independent of the assumed $^1J(^{13}C-^1H)$ values.

Figure 14 shows the DEPT pulse sequence and vector diagram of an AX system corresponding to a CH system, where A and X are ^1H and ^{13}C nuclei, respectively.[22] After the first 90°(x) pulse in the $A(^1H)$ region (a), the transverse magnetization of $A(^1H)$ is modulated by coupling to the $X(^{13}C)$ nucleus, resulting in a doublet with coupling constant $J(^{13}C-^1H)$. After time $t = \frac{1}{2}J$ sec, a phase difference of 180° exists between the vectors of the doublet (b). A 180°(x) pulse in the $A(^1H)$ region is used to refocus phase error caused by inhomogeneity of the magnetic field. At the same time, a 90°(x) pulse in the $X(^{13}C)$ region results in the transverse magnetization of $X(^{13}C)$. Since the magnetization vector of neither $A(^1H)$ or $X(^{13}C)$

[36] G. A. Morris and R. Freeman, *J. Am. Chem. Soc.* **101,** 760 (1979).

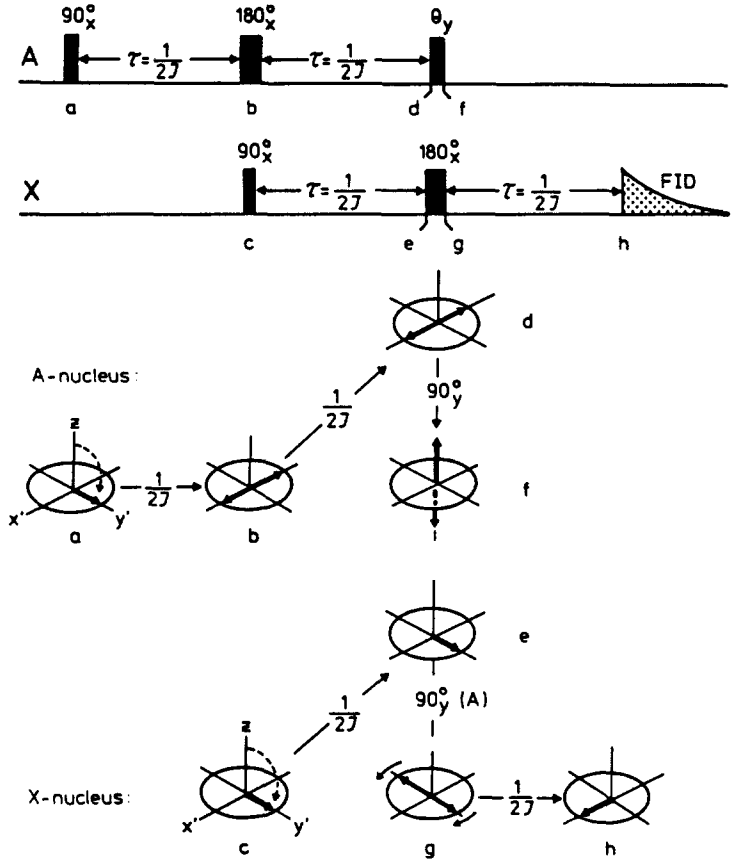

FIG. 14. DEPT pulse sequence and vector diagram for an AX system.[22] (Reproduced by permission of VCH Verlagsgesellschaft, Weinheim, Federal Republic of Germany.)

is present along the z'-axis in the double rotating frame of reference, $A(^1H)$ and $X(^{13}C)$ are practically decoupled. During the next $\frac{1}{2}J$-sec period, both vectors are stationary in their rotating frames of reference (d and e, respectively). At $t = 2(\frac{1}{2}J)$ sec, a 90°(y) pulse ($\theta = 90°$) in the $A(^1H)$ region polarizes the magnetization of A(f). At the same time, this causes polarization of the magnetization of $X(^{13}C)$ (g). The reestablishment of magnetization along the z'-axis in the $A(^1H)$ region leads to refocusing of the vectors of $X(^{13}C)$ via spin–spin coupling in the last $\frac{1}{2}J$-sec period (h). The magnetization of $X(^{13}C)$ can be detected with uniform phase as a doublet with coupling constant $J(^{13}C-^1H)$ or as singlet with simultaneous ^1H decoupling at $t = 3(\frac{1}{2}J)$ sec until the end of the data acquisition time. After a recycling time D_1 sec, the pulse sequence is repeated.

The DEPT experiments for lignin preparation are conducted at 50° in DMSO-d_6 solution using the microprogramming facilities of the ASPECT 2000 pulse programmer,[37] provided with a Bruker WM 200 (or WM 250) NMR spectrometer, according to the following sequences (also see Fig. 16) [Note: ^{1}H decoupler is turned on at the time $t = D_2$, i.e., during data acquisition time (FID), and turned off immediately after FID.]:

$$\begin{array}{ll} ^1\text{H} & 90°(\text{x}) - D_2 - 180°(\text{x}) - D_2 - \theta°(\text{y}) - D_2 \\ ^{13}\text{C} & \qquad\qquad 90°(\text{x}) - D_2 - 180°(\text{x}) - D_2 \\ & \qquad\qquad\qquad\qquad - \text{FID} - D_1 \end{array}$$

where $D_2 = 1/(2J_{CH})$ and D_1 = recycling time. For a lignin preparation, D_2 is obtained from an average value of $^1J(^{13}\text{C}-^1\text{H}) = 150$ Hz, e.g., $D_2 = 1/300$ sec. D_1 must be chosen so that $D_1 > T_1$ of ^{1}H, i.e., $D_1 = 3$ sec. Spectra are obtained from three different values of $\theta°(\text{y})$ pulse: $\theta_1 = \pi/4$ (45°), $\theta_2 = \pi/2$ (90°), and $\theta_3 = 3\pi/4$ (135°).[20,35] The CH, CH_2, and CH_3 subspectra are edited by linear combination of the spectra obtained with the three values of ($\theta°$, y) pulse as follows:

$$\text{CH subspectrum} \quad \theta_2 - z(\theta_1 + x\theta_3) \tag{34a}$$

$$\text{CH}_2\text{ subspectrum} \quad \tfrac{1}{2}(\theta_1 + x\theta_3) \tag{34b}$$

$$\text{CH}_3\text{ subspectrum} \quad \tfrac{1}{2}(\theta_1 + x\theta_3) - y\theta_2 \tag{34c}$$

where θ_1, θ_2, and θ_3 denote the spectra obtained with the three values of $\theta°(\text{y})$ pulse, $\theta_1 = \pi/4$, $\theta_2 = \pi/2$, and $\theta_3 = 3\pi/2$, respectively. Theoretically, $x = 1$, $y = 0.71$, and $z = 0$.[20] However, the parameters x, y, and z are experimentally determined by obtaining the optimal cancellation of unwanted signals in the subspectra using the corresponding IGD spectrum of the lignin as reference.

The ^{13}C 90°pulse has a pulse width of 14.5 μsec using the ASPECT pulse programmer. As the ^{1}H $\theta°(\text{y})$ pulses are never homogeneous, to calibrate the ^{1}H 90° pulse, the pulse width is adjusted so that the CH_2 signals of the sample are nullified with the $\frac{1}{2}J = D_2$ sec time periods. The calibration usually results in a pulse width of 31–36 sec for the ^{1}H 90° pulse. The pulse widths for the ^{1}H 45 and 135° pulses are directly obtained from the ^{1}H 90° pulse.

Figures 15 and 16 show CH, CH_2, and CH_3 subspectra of MWLs from birch and *B. polycarpa* obtained by the DEPT technique under the aforementioned operational conditions, respectively. Figure 17 shows a quater-

[37] M. R. Bendall, D. T. Pegg, D. M. Doddrell, and W. E. Hull, "DEPT Bruker Information Bulletin." Bruker Analytische Messtechnik, Karlsruhe, Federal Republic of Germany, 1982.

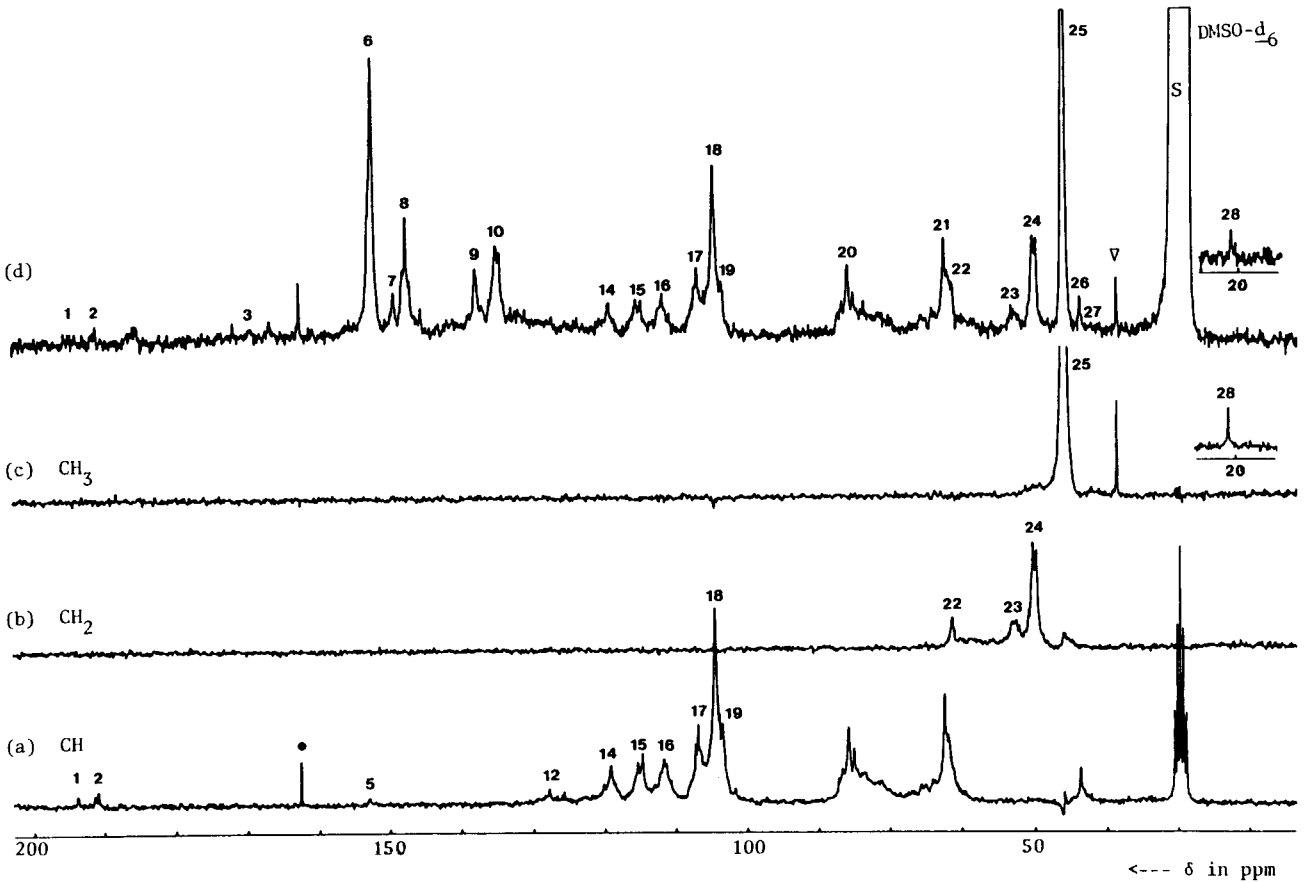

FIG. 15. DEPT-edited ^{13}C NMR spectra of MWL from birch *(B. verrucosa)*. (a) CH signals, (b) CH_2 signals, (c) CH_3 signals, and (d) inverse gated decoupled spectrum (● and ▽) Contaminant.[24] (Reproduced by permission of Huthig & Wepf Verlag, Basel, Switzerland.)

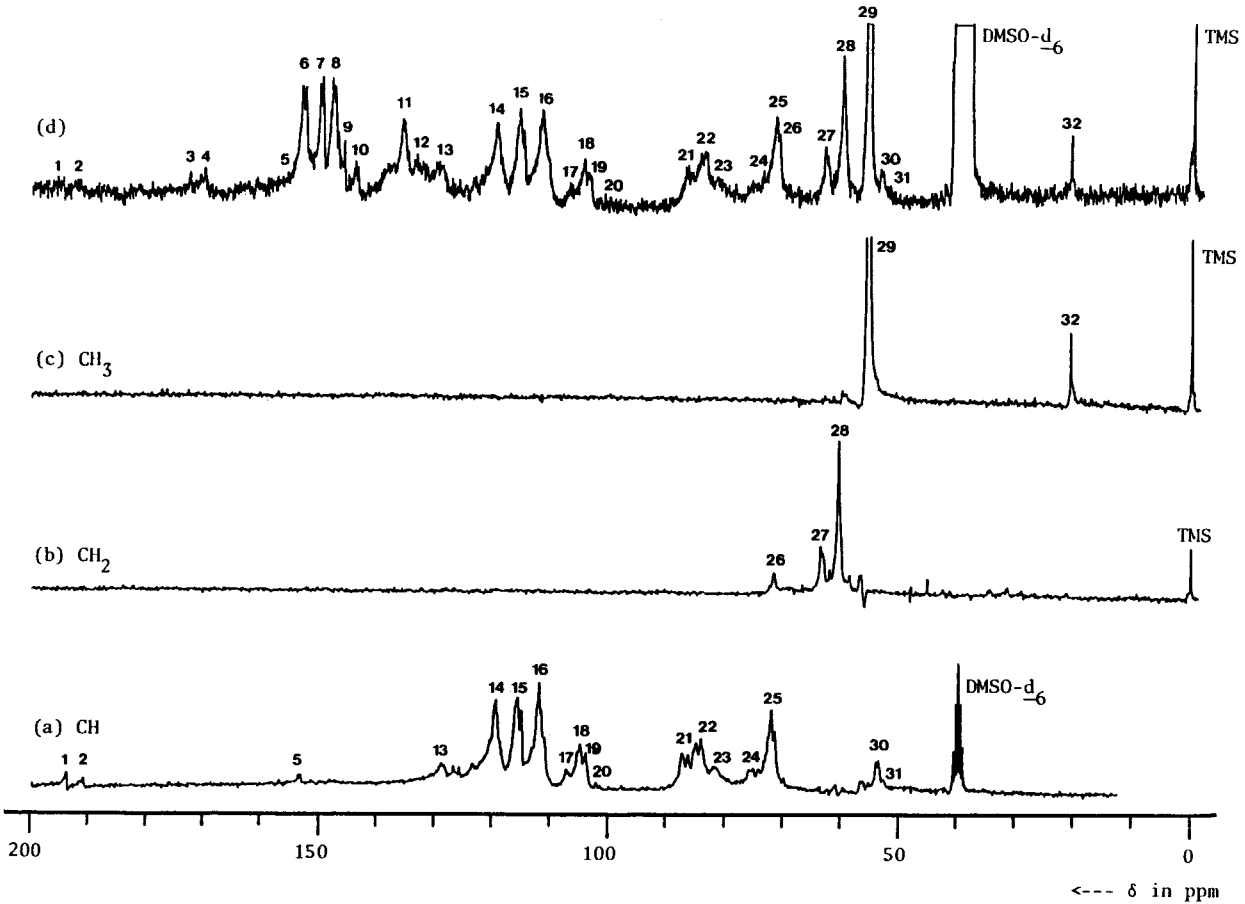

FIG. 16. DEPT-edited ^{13}C NMR spectra of MWL from *B. polycarpa*. (a) CH signals, (b) CH_2 signals, (c) CH_3 signals, and (d) inverse gated decoupling spectrum.

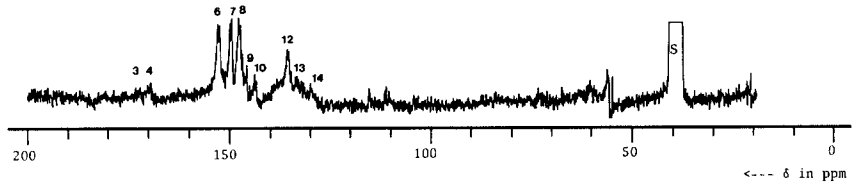

FIG. 17. Difference spectrum of MWL by subtracting the DEPT-edited subspectra for CH, CH_2, and CH_3 signals from the inverse gated decoupled spectrum.

nary C subspectrum obtained by subtraction of Σ DEPT (CH + CH_2 + CH_3) subspectra from the IGD ^{13}C NMR spectrum of the MWL from *B. polycarpa.*

Interpretation of ^{13}C NMR Spectra of Lignins

As compared to the corresponding ^{1}H NMR spectra, both routine and quantitative ^{13}C NMR spectra of lignins have considerably larger spectral widths, i.e., larger chemical shift range, and better resolution of signals due to proton decoupling. Thus, these spectra provide much more useful information for characterization of lignins than the corresponding ^{1}H NMR spectra. However, interpretation of the spectra depends entirely on the ^{13}C NMR spectra data of lignin model compounds. Table III summarizes chemical shifts of ^{13}C nuclei in the major lignin substructures and possible contaminants.

The ^{13}C NMR spectra of MWL from birch *(B. verrucosa)* including the DEPT subspectra have been analyzed.[24,31,33] The results are given in Table IV. In this section, the spectra of MWL from wood of *B. polycarpa* will be interpreted semiquantitatively. As described previously, the lignin contains about 5.6% carbohydrate and has a C_9 unit formula of $C_9H_{6.59}O_2(H_2O)_{0.89}(OCH_3)_{1.13}$ (C_9 unit weight, 197.83) after correction of carbohydrates (for analytical data, see chapter [14], Table I, in this volume). An examination of the quantitative ^{13}C NMR spectrum of MWL (Fig. 13) reveals that the MWL indeed contains carbohydrates as evidenced by the presence of signals 4, 20, 24, and 32 at δ 169.6, 101.6, 76–73, and 20.9 ppm corresponding to acetyl C=0, C—1 of xylan, C—2 ~ C—4 of xylan, and acetyl CH_3, respectively. The spectrum shows that the lignin is of the guaiacylsyringyl type. The presence of guaiacylpropane structures is evidenced by signals 14, 15, and 16 at δ 119.6, 115.8, and 112.2 ppm corresponding to C—6, C—5, and C—2 of guaiacyl group, respectively. In contrast to the rather weak signal 9 at δ 145.6 ppm corresponding to C—4 of guaiacyl group, signals 7 and 8 at δ 149.9–149.4 and 147.7–147.2 ppm are very strong. Since signals 7 and 8 correspond to C—3 and

TABLE III
CHEMICAL SHIFTS FOR ^{13}C NUCLEI IN LIGNINS[a]

Chemical shift (δ in ppm)	Type of ^{13}C nucleus
194	C=O in Ar—CH=CH—CHO and Ar—COR
192–191.5	C=O in Ar—CHO
172.1	COOH in aliphatic acid
169.5–169.0	Acetyl C=O in acetylated xylose and in xylan
167.2	COOH in Ar—COOH
165.2	C=O in *p*—hydroxybenzoate
162.0	C-4 in *p*—hydroxybenzoate
153–152	C-3 in etherified biphenyl (5–5)
	C-3/C-5 in S *β-O*-4 (S etherified)
	C-α in Ar—CH=CH—CHO
149.2	C-3 in G *β-O*-4 (G etherified)
147.5–147	C-3 in G nonetherified
	C-4 in G *β-O*-4 (G etherified)
	C-3/C-5 in S nonetherified
145.3	C-4 in G nonetherified
143.3	C-4 in phenylcoumaran (*β*-5)
	C-4 in 5–5 etherified
141.5	C-1/C-4 in 5–5 nonetherified
137.9	C-4 in S nonetherified
135–134	C-1 in G and S etherified
134–132	C-1 in G and S nonetherified
131.4	C-2/C-6 in *p*—hydroxyphenylbenzoate
129–128	C-β in Ar—CH=CH—CHO
	CH=CH in Ar—CH=CH—CH_2OH
120.5	C-1 in *p*—hydroxybenzoate
120–119	C-6 in G etherified and nonetherified
115.5–115	C-5 in G etherified and nonetherified
112–111	C-2 in G etherified and nonetherified
107–106	C-2/C-6 in S with α-C=O
104.5–103.5	C-2/C-6 in S
102–101	C-1 in xylose unit of xylan
86–85	C-β in *β-O*-4
83.6	C-β in *β-O*-4 with α-C=O
72.2	C-α in *β-O*-4
69.7	C-5 in xylose unit of xylan
63.2	C-γ in *β-O*-4 with α—C=O
62.7	C-γ in *β*-5
60.1–59.6	C-γ in *β-O*-4
55.5–56	OCH_3 in Ar—OCH_3
53.8	C-β in β–β
53.4	C-β in β–5

[a] G, Guaiacyl; S, syringyl.

TABLE IV
ASSIGNMENTS OF SIGNALS IN ^{13}C NMR SPECTRUM OF MWL FROM BIRCH (*Betula verrucosa*)[a]

ignal	δ (ppm)	Assignment
1	194	C═O in Ar—CH═CH—CHO
2	191.6	C═O in Ar—CHO
3	165–172	COOH in aromatic and aliphatic esters
5	152.6	C-α vinylic in cinnamaldehyde
6	152.1	C-3/C-5 in β-*O*-4 (S etherified)
7	149.2	C-3 in G β-*O*-4 (S etherified)
8	147.4	C-3 in G; C-4 in G β-*O*-4; C-3/C-5 in S nonetherified
9	138	C-1/C-4 in S etherified
10	134.4	C-1 in G etherified; C-4 in β–β
12	129.3	C-β vinylic in cinnamaldehyde
14	120.4	C-6 in G etherified and nonetherified
15	115.1	C-5 in G etherified and nonetherified
16	111.7	C-2 in G etherified and nonetherified
17	106.8	C-2/C-6 in S with α-C═O
18	104.4	C-2/C-6 in S β-*O*-4 and with CHOH
19	103.6	C-2/C-6 in S
20	85.8–82	C-β in β-*O*-4
21	72.2	C-α in β-*O*-4
22	71.8	C-γ in syringaresinol and/or pinoresinol
23	62.9	C-γ in β-*O*-4 with β-C═O; in β-5, in β-1
24	60.1–59.6	C-γ in β-O-4
25	55.9	—OCH_3
26	53.4	C-β in syringaresinol unit
27	Sh. 52.7	C-β in phenylcoumaran unit
28	21.0	γ-CH_3 adjacent to a C-β-OH and/or acetyl groups in xylan

[a] G, Guaiacyl; S, syringyl; Sh, shoulder. From Bardet *et al.*[24]

C—4 of 4—*O*—alkylated guaiacyl group, the guaiacyl moieties must be present in the lignin in the form of 4—*O*—alkyl ethers. Moreover, the 4—*O*—alkaylated guaiacyl moieties seem to be present in the lignin predominantly in the form of β—*O*—4 substructures because of the presence of relatively strong signals 22, 25, and 28 at δ 84.6, 71.8, and 60.2 ppm. These signals correspond to C—β, C—α, and C—γ of β—*O*—4 substructure, respectively. The presence of a syringylpropane structure is evidenced by signals 18 and 19 at δ 104.9 and 103.7 ppm, both corresponding to C—2/C—6 of syringl group; in addition to signal 6 at δ 152.6–152.3 ppm corresponding to C—3/C—5 of 4—*O*—alkaylated syringl group. The presence of the signal 21 at δ 87.0 ppm in addition to the signals 25 and 26 indicates further that 4—*O*—alkaylated syringlpropane units are present in the lignin mostly in the form of β—*O*—4 substructure. Signals 30 and 31 at δ 53.4 and 53.4 ppm indicate the

presence of $\beta-\beta$ and $\beta-5$ substructures in the lignin, respectively. The assignment of signals are given in Table V.

The aromatic region of the spectrum is chosen as standard to analyze the spectrum quantitatively, since the region does not contain the signals of carbohydrate contaminants. The DEPT CH subspectrum (Fig. 16a) indi-

TABLE V

ASSIGNMENTS OF SIGNALS IN ^{13}C NMR SPECTRUM OF MWL FROM WOOD OF *Bischofia polycarpa*[a]

Signal	δ (ppm)	Assignment
1	194.0	C=O in Ar—CH=CHO
2	191.6	C=O in Ar—CHO
3	172	COOH in aliphatic acid
4	169.6	Acetyl C=O in acetylated xylose unit in xylan
5	152.9	C-α in Ar—CH=CH—CHO
6	152.9–152.3	C-3 in etherified biphenyl (5–5) C-3/C-5 in S β-*O*-4 (S etherified)
7	149.2–149.4	C-3 in G β-*O*-4 (G etherified)
8	147.7–147.2	C-3 in G nonetherified C-4 in G β-*O*-4 (G etherfied C-3/C-5 in S nonetherified) C-3/C-5 in S nonetherified
9	145.6	C-4 in G nonetherified
10	143.2	C-4 in phenylcoumaran C-4 in 5–5 etherified
11	135.6	C-1 in G etherified
12	135–131	C-1 in G and S nonetherified
13	130–129	CH=CH in Ar—CH=CH—CH_2OH: C-β in Ar—CH=CH—CH(
14	119.0	C-6 in G etherified and nonetherified
15	115.8	C-5 in G etherified and nonetherified
16	112.2	C-2 in G etherified and nonetherified
17	106.5	C-2/C-6 in S with α—C=O
18	104.7	C-2/C-6 in S
19	103.7	C-2/C-6 in S
20	101.6	C-1 in xylose unit of xylan
21	87.0	C-β in S β-*O*-4
22	84.6	C-β in G β-*O*-4
23	81.2	—
24	76–73	C-2/C-3/C-4 in xylose unit of xylan
25	71.6	C-α in β-*O*-4
26	71.0	C-γ in G and S $\beta-\beta$
27	62.9	C-γ in β-*O*-4 with α—C=O; in β-5, in β-1
28	60.2	C-γ in β-*O*-4
29	55.8	—OCH_3 in Ar—OCH_3
30	53.8	C-β in $\beta-\beta$
31	53.4	C-β in β-5
32	20.4	

[a] G, Guaiacyl; S, syringyl. From Robert *et al.*[29]

cates the presence of cinnamaldehyde and cinnamyl alcohol structures as evidenced by signals 1, 5, and 13 at δ 194.0, 152.9, and 129.7–129.4 ppm, respectively. From the integral, the quantity of cinnamaldehyde and cinnamyl alcohol is estimated to be each in the order of about 0.02 U/1 aromatic ring. Consequently, the integral of the aromatic region should correspond to 6.08 carbons. Since the total integral of the region is 56, the integral for one carbon is 56/6.08 = 9.21. The DEPT CH subspectrum also shows that the tertiary aromatic carbon region is δ 128–103 ppm excluding 0.08 vinylic carbons. The region δ 128–103 ppm is the syringyl C—2/C—6 region. The quaternary carbon region is δ 156–128 ppm including 0.08 vinylic carbons. The total integral of each region is then divided by the factor for one carbon, i.e., 9.21, to obtain the total number of carbons per one aromatic ring in the region. The results are given in Table VI.

It is obvious that the total number of carbons/benzene ring in the methoxyl region corresponds to the number of methoxyl groups per C_9 unit. Thus, the methoxyl content is 1.15/C_9 unit. This is a good agreement with 1.13/C_9 unit obtained from the elemental analysis. Since one syringyl group always has two C—2/C—6 carbons, the approximate ratio of syringylpropane units/C_9 unit can be obtained by dividing the total number of carbons in the spectral region by 2, i.e., 0.36/2 = 0.18. Assuming that no *p*-hydroxyphenylpropane units are present in the lignin, then the ratio of syringylpropane units to guaiacylpropane units in the lignin is 0.18:0.82/C_9 unit. The number of methoxyl groups/C_9 unit would then be $2 \times 0.18 + 0.82 = 1.18/C_9$ unit. The methoxyl content thus obtained is somewhat higher than the experimental value of 1.13/C_9 unit and the value 1.15/C_9 unit obtained from the methoxyl region. The excess value proba-

TABLE VI
INTEGRAL OF SPECTRAL REGIONS IN ^{13}C NMR SPECTRUM OF MWL FROM *Bischofia polycarpa*[a]

Spectral region	Chemical shift range [δ (ppm)]	Integral	Number of carbons per one benzene ring
Quaternary C.[b]	156–128	33.0	3.58
Tertiary C	128–103	23.0	2.50
Syringyl C-2/C-6	108–103	3.3	0.36
Side chain[c]	90– 57.5	28.6	3.11
Methoxy	57.5– 54.5	10.6	1.15
C-β of β–β and β-5	54.5– 53.0	0.8	0.09

[a] Factor for one carbon = 56/6.08 = 9.21. From Robert *et al.*[29]
[b] Includes four vinylic carbons.
[c] Excludes C-β of β–β and β-5 substructures.

bly is due to the presence of diphenyl ether (4—*O*—5) substructure. The chemical shift of C—2 and C—6 in 5—aroxyguaiacylpropane is in the chemical shift range δ 110–103 ppm. Thus, the number of 4—*O*—5 substructures would be $1.18-1.15 = 0.03/C_9$ unit. On the basis of $KMnO_4$–$NaIO_4$ oxidation, the amount of 4—*O*—5 substructure in lignin has been estimated to be in the order of $0.03-0.05/C_9$ unit.[38] Thus, the value for 4—*O*—5 substructure obtained here is rather reasonable, and the methoxyl content is about $1.15/C_9$ unit. The lignin then consists of guaiacylpropane and syringylpropane units in the molar ratio of 0.85:0.15. Assuming that the lignin does not contain aromatic ring condensed units, then the number of tertiary carbons must be $0.85 \times 3 + 0.15 \times 2 = 2.85/C_9$ unit. From the tertiary carbon spectral region, a value of $2.50/C_9$ unit is obtained. The degree of condensation for aromatic ring is then $2.85 - 2.50 = 0.35/C_9$ unit.

The signal 6 has integral 4.6 corresponding 0.5 carbons/C_9 unit. Since the signal arises from C—3/C—5 of 4—*O*—alkylated syringyl group and C—3 of 4,4′—*O*—dialkylated biphenyl (5–5) substructure, the number of carbons for the *O*-dialkylated 5–5 substructure can be estimated by the difference between the number of carbons under the signal 6 and the number of C—3/C—5 carbons in the syringyl units. Assuming that about 90% of the latter is involved in β—*O*—4 substructure, the number of carbons for C—3 of the 4,4′-*O*-dialkylated biphenyl (5–5) substructure is $0.5 - 0.15 \times 2 \times 0.9 = 0.23/C_9$ unit. Since the 5–5 substructure is a symmetric dimer, the number of the etherified 5–5 substructure is about $0.11/C_9$ unit. Similarly, the integral for signal 7 is 4.0 corresponding to 0.43 carbons/C_9 unit. Since the signal is characteristic of the C—3 of 4—*O*—alkaylated guaiacylpropane unit, the number of the unit is about $0.43/C_9$ unit. These units are involved in either β—*O*—4 or α—*O*—4 substructures; usually about 80% of these units are present in the form of β—*O*—4. Thus, the number of etherified guaiacyl type β—*O*—4 substructures would be about $0.34/C_9$ unit and that of α—*O*—4 substructures would be about $0.09/C_9$ unit. The number of syringyl type β—*O*—4 substructures would be about $(0.30 \times 0.90)/2 = 0.13/C_9$ unit.

[38] M. Erickson, S. Larsson, and G. Miksche, *Acta Chem. Scand.* **27**, 903 (1973).